Octakis(2-pyridyl)porphyrazine and Its Neutral Metal Derivatives: UV-Visible Spectral, Electrochemical and Photoactivity Studies

Fabiola Sciscione,[&] Lei Cong,[§] Maria Pia Donzello,*,[&] Elisa Viola,[&] Claudio Ercolani,[&] and Karl M. Kadish*,[§]

[&] Dipartimento di Chimica, Università di Roma Sapienza, P.le A. Moro 5, I-00185 Roma, Italy

[§] Department of Chemistry, University of Houston, Houston, Texas, 77204-5003, USA

Abstract

Tetrapyrrolic porphyrazine macrocycles with externally appended 2-pyridyl rings were synthesized and characterized as to their spectroscopic, electrochemical and photophysical properties. The investigated compounds are represented as $[Py_8PzH_2]$, the unmetalated octakis(2-pyridyl)porphyrazine, and the metal complexes $[Py_8PzM]$ where M is $Mg^{II}(H_2O)$, Cu^{II}, Zn^{II} or Co^{II}. The spectroscopic properties and the electrochemical behavior of these compounds were examined in solution of polar (pyridine, DMSO and DMF) and non donor solvents ($CHCl_3$, CH_2Cl_2) and the data compared with those obtained from earlier studies on the related tetrapyrazinoporphyrazines, $[Py_8TPyzPzM]$, and the tetraquinoxalinoporphyrazines, $[Py_8QxPzM]$, also bearing externally 2-pyridyl rings, and characterized by a more extended central π-conjugated macrocyclic framework. The newly synthesized porphyrazines possess good solubility and are present in their monomeric form in all the examined solvents as shown by UV-visible spectra. The unmetalated species and metal derivatives undergo multiple one-electron reductions within the potential range of the non-aqueous examined solvents. The derivatives with non-redox active metal centers could accept four electrons on the conjugated macrocycle while the Co^{II} complex was characterized by a single one-electron oxidation and five reductions in DMSO. The photosensitizer activity for the generation of singlet oxygen was also examined for the $Mg^{II}(H_2O)$ and Zn^{II} complexes in DMF, with measured Φ_Δ values being, respectively, 0.42 and 0.64, this latter value indicating the Zn^{II} species as being a promising material for use as anticancer agent in Photodynamic therapy (PDT).

1

Introduction

The synthesis and characterization of tetrapyrazinoporphyrazines with externally appended 2-pyridyl rings was recently reviewed.[1] An example of these compounds is represented by derivatives having the formula [Py$_8$TPyzPzM] where Py$_8$TPyzPz represents the tetrapyrazinoporphyrazine dianion and M is a divalent metal ion (Figure 1B). One goal of the earlier studies was to explore their potential as photosensitizers in photodynamic therapy (PDT)[2] and to define possible interactions of these compounds with a telomeric G-4 quadruplex structure[3] and a ds model of B-DNA.[4]

Based on measurements of UV-visible spectral and electrochemical data, it was established that the [Py$_8$TPyzPzM] complexes bearing annulated electron-withdrawing pyrazine rings exhibit remarkably higher electron deficient properties than the related phthalocyanine analogs [PcM] (Pc = phthalocyaninato anion) which contain ß,ß-fused benzene rings.[5] This is clearly evidenced by the observed hypsochromic shift of the Q band positions and the easier uptake of electrons for these compounds.

As part of our ongoing studies involving porphyrazines, we wished to explore the influence of reducing or extending the central macrocyclic framework, with the aim of changing the size of the π-electron delocalized system. Accordingly, macrocycles having the formula [Py$_8$PzM] (Figure 1A) and [Py$_8$QxPzM] (Figure 1C) were synthesized. The compounds in Figure 1A can be formally thought of as being derived from [Py$_8$TPyzPzM] by removing the pyrazine rings from the compounds in Figure 1B, while the complexes of formula [Py$_8$QxPzM] (Figure 1C) carry additional benzene rings interposed between the four pyrazine rings and the four linked pyrroles. Template macrocyclization reactions enabled synthesis of the two new species as Mg^{II} derivatives, ie. [Py$_8$PzMg(H$_2$O)] and [Py$_8$QxPzMg(H$_2$O)],[6] and the examined UV-visible spectra of these compounds in dimethylformamide indicate that the Q band maximum moves systematically towards the red as the macrocycle π-system expands, ie. 635 → 658 → 759 nm for the sequence [Py$_8$PzMg(H$_2$O)] → [Py$_8$TPyzPzMg(H$_2$O)] → [Py$_8$QxPzMg(H$_2$O)]. TDDFT calculations of absorption spectra were made for the corresponding water-free model compounds,6 and a good agreement was found between theoretical calculations and the experimental data, thus providing a satisfactory description of the UV-visible spectra as determined by the electronic structural changes along the series.
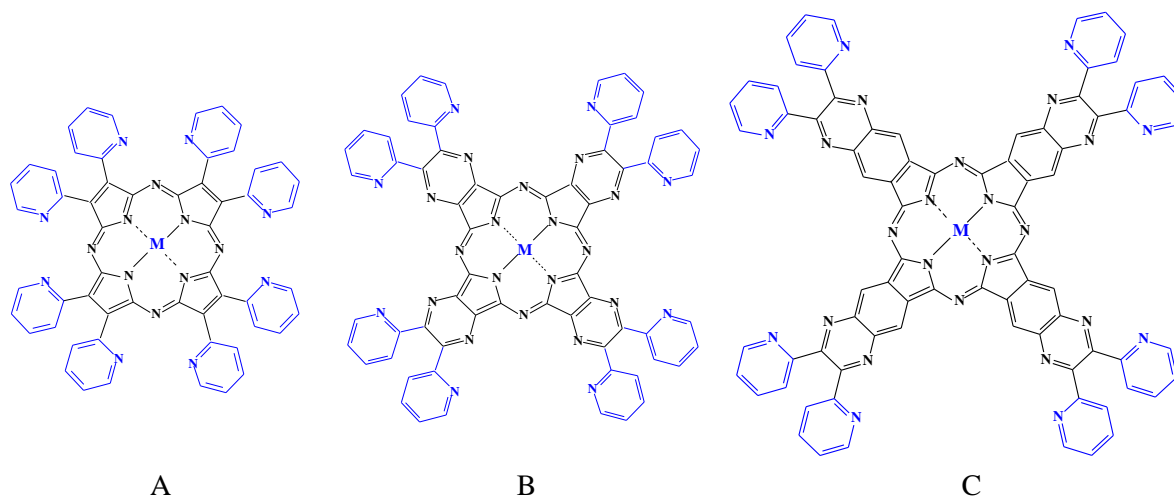
Figure 1. Schematic representation of (A) [Py$_8$PzM], (B) [Py$_8$TPyzPzM], and (C) [Py$_8$QxPzM].

A further aspect of our work recently focused on metal derivatives with the smaller macrocycle bearing the 2-pyridyl groups directly attached to each of the four internal pyrrole rings, ie [Py$_8$PzM] (Figure 1A). Worthy of note is the fact that the Zn^{II} complex in the series, [Py$_8$PzZn], could be obtained from the corresponding Mg^{II} analog under mild experimental conditions via a transmetalation process in glacial CH$_3$COOH containing Zn(OAc)$_2$·2H$_2$O. The same type of reaction was attempted for the synthesis of Co^{II} and Cu^{II} complexes but this did not lead to satisfactory results since analytically pure compounds were not obtained. This suggested that a synthesis of the unmetalated [Py$_8$PzH$_2$] macrocycle was needed and could potentially open up perspectives for formation of a new series of compounds with different central metal ions. As described in the current manuscript, the octakis(2-pyridyl)porphyrazine, [Py$_8$PzH$_2$], was successfully obtained from its Mg^{II} complex and was used for the synthesis of its Co^{II} and Cu^{II} derivatives. The Zn^{II} complex was also prepared via a conversion of [Py$_8$PzH$_2$] to [Py$_8$PzZn] as an alternative to the transmetalation process.

Synthetic procedures are now reported in the current manuscript for all of the species represented as [Py$_8$PzM] (M = 2H^{I}, Mg^{II}(H$_2$O), Zn^{II}, Co^{II}, Cu^{II}), along with IR, UV-visible, NMR and electrochemical characterization of the compounds. The photoactivity of the Mg^{II} and Zn^{II} species is also reported in a non-aqueous solvent (DMF) with the goal of using these metal complexes as

3

sensitizers for the generation of singlet oxygen, $^1O_2$, a topic of interest in PDT, with positive results as to their response in terms of quantum yields values (Φ_Δ).

Experimental Section

Solvents and reagents were used as purchased, unless otherwise specified. Pyridine, dried by refluxing over CaO, and dimethyl sulfoxide (DMSO, RPE C. Erba), freshly distilled over CaH_2, were used for the spectroscopic measurements. Methanol was dried over sodium and freshly distilled before use. The already reported[7] synthesis of 1,2-di(2-pyridyl)-1,2-dicyanoethylene, $[(CN)_2Py_2Et]$, was slightly modified as recently described.[6] The Mg^{II} complex $[Py_8PzMg(H_2O)]$ was prepared following the reported procedure,[6] slightly modifying its purification (checked by UV-visible spectra; see Figure S1) which was performed by column chromatography using alumina (Merck, activated, basic, 0.063-0.200 microns) as the solid phase and $CHCl_3$ as first eluant, followed by the use of a gradient from 5% to 20% of CH_3OH in $CHCl_3$. Elemental analysis: Calcd for $[Py_8PzMg(H_2O)]\cdot 4H_2O$, $C_{56}H_{42}MgN_{16}O_5$: C, 64.47; H, 4.06; N, 21.48. Found: C, 64.54; H, 4.22; N, 20.98%. ^{1}HNMR (DMSO-d_6, 300 K): δ/ppm = 8.775 (d, J = 4.4 Hz, 8 H; α,α'), 7.590 (d,d,d, J = 6.9; 5.6; 1.0 Hz, 8 H; β,β'), 8.205 (d,d,d, J = 7.8; 7.7; 1.7 Hz, 8 H; γ,γ'), 8.910 (d, J = 7.8 Hz, 8 H; δ,δ'). ^{13}C NMR (DMSO-d_6, 300 K)::δ/ppm = 154.4 (2-pyridyl ring: quaternary C), 150.2 (α,α'), 123.7 (β,β'), 136.7 (γ,γ'), 129.7 (δ,δ'); signals of the pyrrol C atoms are not detectable due to low intensity.

Synthesis of $[Py_8PzH_2]\cdot 5H_2O$. $[Py_8PzMg(H_2O)]\cdot 4H_2O$ (49 mg, 0.047 mmol) was added to glacial acid acetic CH_3COOH (1 mL) in a 10 mL flask and the mixture was kept at room temperature under stirring for 5 h. The obtained solution was poured in air into a vessel and the solvent was left to evaporate completely. The solid residue was dissolved in water and the resulting acid solution was neutralized by dropwise addition of a solution of 0.1 M NaOH. The bluish precipitate was isolated by centrifugation, washed with water until neutrality and brought to constant weight under vacuum (10^{-2} mmHg; 31 mg, yield 62%). Calcd for $[Py_8PzH_2]\cdot 5H_2O$, $C_{56}H_{44}N_{16}O_5$: C, 65.87; H, 4.34; N, 21.95. Found: C, 65.47; H, 3.59; N, 21.42%. IR (KBr, cm^{-1}): 3425 (broad), 3293 (w, ν_{NH}), 1584 (s), 1562 (m), 1461 (s), 1421 (s), 1286 (w), 1243 (vvw), 1178 (w-m), 1150 (m), 1121 (w-m), 1095 (m), 1048 (w-m),

998 (vvs), 976 (vs), 860 (m-s), 829 (vvw), 799 (w), 771 (m), 739 (m), 710 (m-s), 676 (w), 621 (w), 595 (m), 569 (vvw), 523 (vw), 444 (vw), 409 (vw), 401 (w). ^{1}H NMR (CDCl$_3$, 300 K): δ/ppm = 8.811 (d, J = 4.8 Hz, 8H; α,α'), 7.460 (d,d,d, J = 7.7; 4.8; 1.0 Hz, 8H; β,β'), 7.959 (d,d,d, J = 7.7; 7.7; 1.8 Hz, 8H; γ, γ'), 8.771 (d, J = 7.7 Hz, 8H; δ,δ'), -1.423 (s, 2H (NH)). ^{13}C NMR (CDCl$_3$, 300 K): δ/ppm = 152.9 (2-pyridyl ring: quaternary C), 149.5 (α,α'), 122.7 (β,β'), 135.6 (γ,γ'), 129.0 (δ,δ'); signals of the pyrrol C atoms are not detectable due to low intensity.

Synthesis of [Py$_8$PzZn]·7H$_2$O via a transmetalation process. [Py$_8$PzMg(H$_2$O)]·5H$_2$O (53.8 mg, 0.051 mmol) and Zn(OAc)$_2$·2H$_2$O (34.3 mg, 0.16 mmol) were suspended in glacial CH$_3$COOH (2 mL). The suspension was kept under stirring at room temperature for 5 h. The mixture was then poured into a vessel and the solvent was left to evaporate completely. The solid residue was dissolved in water and the resulting acid solution was neutralized by dropwise addition of a solution of 0.1 M NaOH. The formed bluish precipitate was isolated by centrifugation, washed with water and brought to constant weight under vacuum (10^{-2} mmHg; 48.6 mg, yield 84.3%). Calcd. for [Py$_8$PzZn]·7H$_2$O, C$_{56}$H$_{46}$N$_{16}$O$_7$Zn: C, 60.03; H, 4.14; N, 20.00; Zn, 5.83. Found: C, 60.04; H, 2.89; N, 19.77; Zn 6.23%.IR (KBr, cm^{-1}): 3380 (broad), 1585 (vs), 1561 (w), 1513 (w), 1463 (m-s), 1423 (m), 1367 (w-m), 1286 (w-m), 1241 (vw), 1149 (vs), 1092 (m), 1047 (m), 1005 (vvs), 983 (s), 880 (s), 834 (m), 753 (w), 721 (wm), 697 (w), 604 (m), 497 (vw).

Synthesis of [Py$_8$PzZn]·3H$_2$O from [Py$_8$PzH$_2$]. [Py$_8$PzH$_2$]·5H$_2$O (14 mg, 0.014 mmol) and Zn(OAc)$_2$·2H$_2$O (9 mg, 0.041 mmol) were suspended in pyridine (1 mL) and the suspension kept under stirring for 3 h at 60 °C. After evaporation of the solvent, the blue-green solid material was washed with water and acetone and brought to constant weight under vacuum (10^{-2} mmHg; 7 mg, yield 43%). Calcd. for [Py$_8$PzZn]·3H$_2$O, C$_{56}$H$_{38}$N$_{16}$O$_3$Zn: C, 64.16; H, 3.65; N, 21.38; Zn, 6.24%. Found: C, 63.76; H, 3.58; N, 21.06 %, Zn, 6.12%.

Synthesis of [Py$_8$PzCo]·6H$_2$O. [Py$_8$PzH$_2$]·4H$_2$O (23 mg, 0.022 mmol) and Co(OAc)$_2$·4H$_2$O (18 mg, 0.072 mmol) were suspended in freshly distilled pyridine (1 mL) and the mixture was kept under stirring for 2 h at 60 °C. After evaporation of the solvent the solid material was washed with water and acetone and brought to constant weight under vacuum (10^{-2} mmHg; 12 mg, yield 50%). Calcd. for

[Py$_8$PzCo]·6H$_2$O, C$_{56}$H$_{44}$CoN$_{16}$O$_6$: C, 61.37; H, 4.05; N, 20.45; Co, 5.38. Found: C, 61.21; H, 3.80; N, 20.39; Co, 5.38%. IR (KBr, cm^{-1}): 3436 (broad), 1601 (w), 1584 (w), 1503 (w-m), 1466 (w), 1421 (w-m), 1370 (w), 1329 (vw), 1288 (vw), 1173 (m), 1152 (vw), 1104 (vw), 10534 (vw), 1015 (s), 987 (vw), 901 (w), 845 (w), 800 (vw), 777 (vvw), 745 (w), 529 (w-m), 513 (w-m).

Synthesis of [Py$_8$PzCu]·4H$_2$O. [Py$_8$PzH$_2$]·4H$_2$O (30 mg, 0.029 mmol) and Cu(OAc)$_2$·H$_2$O (18 mg, 0.09 mmol) were suspended in freshly distilled pyridine (1 mL) and the mixture kept under stirring for 2 h at 60 °C. After evaporation of the solvent the solid material was washed with water and acetone and brought to constant weight under vacuum (10^{-2} mmHg; 21 mg, yield 65%). Calcd. for [Py$_8$PzCu]·4H$_2$O, C$_{56}$H$_{42}$CuN$_{16}$O$_5$: C, 63.18; H, 3.79; N, 21.05; Cu, 5.87. Found: C, 63.55; H, 4.02; N, 20.76; Cu, 5.97 %. IR (KBr, cm^{-1}): 1584 (m-s), 1564 (w), 1463 (w-m), 1420 (m), 1371 (w), 1287 (w), 1168 (vw), 1151 (w), 1095 (vw), 1051 (w), 1012 (s), 987 (w), 893 (w-m), 840 (w), 800 (vw), 774 (m), 752 (vw), 740 (vw), 669 (vvw), 615 (vvw), 548 (w), 529 (w), 433 (vw).

Electrochemical and Spectroelectrochemical Measurements. Dimethyl sulfoxide (DMSO, 99.9+%) was purchased from Sigma-Aldrich Co. and utilized without further purification. High purity N$_2$ from Trigas was used to deoxygenate the solution before each electrochemical experiment. Tetra-*n*-butylammonium perchlorate (TBAP, 99%) from Fluka Chemika Co. was used as supporting electrolyte and stored under vacuum at 40 °C prior to use.

Cyclic voltammetry (CV) was performed at 298 K with an EG&G model 173 potentiostat coupled with an EG&G Model 175 Universal Programmer. Current-voltage curves were recorded on an Allen Datagraph 1000 or 1100 series X-Y recorder. A three-electrode system was used, consisting of a glassy carbon working electrode, a platinum counter electrode and a saturated calomel reference electrode (SCE). The reference electrode was separated from the bulk solution by a fritted-glass bridge filled with the solvent/supporting electrolyte mixture.

UV-visible spectroelectrochemical experiments were carried out with a home made thin-layer cell which has a light-transparent platinum gauze working electrode. The applied potential was monitored with an EG&G Model 173 potentiostat and UV-visible spectra were recorded on a Hewlett-Packard Model 8453 diode array spectrophotometer.

Singlet oxygen quantum yields measurements in DMF. Measurements of the singlet oxygen quantum yields (Φ_Δ) of the neutral species were carried out in DMF solutions by an indirect and absolute method using 1,3-diphenylisobenzofuran (DPBF) as an $^1O_2$ scavenger, as earlier reported.[8] Solutions of the complexes (ca. 10^{-5}-10^{-6} M) and DPBF (ca. 5 x 10^{-5} M) in DMF or DMF/HCl were irradiated with monochromatic light (Premier LC Lasers/HG Lens, Global Laser) at 635 or 650 nm, values close to the Q-band maximum of each compound. The light intensity was set to 0.300 mW and accurately measured with a radiometer (ILT 1400A/SEL100/F/QNDS2, International Light Technologies).

The Φ_Δ values were obtained from the quantum yield of the photoreaction (Φ_{DPBF}) calculated with respect to the different concentrations of DPBF, on the basis of Equation 1

$$\frac{1}{\Phi_{DPBF}} = \frac{1}{\Phi_\Delta} + \frac{k_d}{k_r}\frac{1}{\Phi_\Delta}\frac{1}{[DPBF]}$$

(1)

where k_d is the decay rate constant of $^1O_2$ in the solvent and k_r is the rate constant of the reaction of DPBF with $^1O_2$. The $1/\Phi_\Delta$ value was obtained as the intercept of the Stern-Volmer plot ($1/\Phi_{DPBF}$ vs $1/[DPBF]$).

Other Physical Measurements. IR spectra of the solid materials as KBr pellets were recorded in the range of 4000-400 cm^{-1} on a Varian 660-IR FT-IR spectrometer. UV-visible solution spectra other than those for spectroelectrochemistry (see above) were recorded with a Varian Cary 5E spectrometer by using 1-cm quartz cuvettes. Thermogravimetric analyses (TGA) were performed on a Stanton Redcroft model STA-781 analyzer under a N_2 atmosphere (0.5 L/min). Elemental analyses for C, H, and N were provided by the "Servizio di Microanalisi" at the Dipartimento di Chimica, Università "Sapienza" (Rome) on an EA 1110 CHNS-O instrument. The ICP-PLASMA analysis of Zn, Co, Cu was performed on a Varian Vista MPX CCD simultaneous ICP-OES. NMR spectral data were obtained by dissolving the samples in 700 μL of DMSO-d_6 (99.9%, Aldrich) or CDCl$_3$ (99.8%, Aldrich) at 27 °C. ^1H and ^{13}C experiments were performed on a Bruker AVANCE AQS 600 spectrometer operating at the proton frequency of 600.13 MHz and equipped with a Bruker multinuclear, z gradient probehead.

[1]H and ^{13}C assignments were obtained by means of HSQC experiments carried out using 1024 data points in the f2 dimension and 512 data points in the f1 dimension, a recycle delay of 1 s, and a coupling constant of 150 Hz.

Results and Discussion

Synthesis and properties of [Py₈PzH₂] and its metal complexes [Py₈PzM] (Mg^{II}(H₂O), Zn^{II}, Co^{II} and Cu^{II}). The purity of the metal free [Py₈PzH₂] and [Py₈PzMg(H₂O)] was established by elemental analyses and the results supported by ^{1}H-NMR spectra taken at room temperature in CDCl₃ and DMSO-*d*₆, respectively (Figure 2; data listed in Experimental Section an in Table 1). The presence of only one set of four resonance peaks for the H atoms of the external 2-pyridyl rings indicates their equivalence in both species and the measured spectra are in line with the spectrum of the [(CN)₂Py₂Et] precursor.[6] For [Py₈PzH₂] a resonance peak assigned to the two protons of the central NH groups is located at -1.423 ppm (Figure 2A, inset). In going from the precursor to either the free ligand or the Mg^{II} complex, the largest low field shift consequent to formation of the macrocycle is observed for the δ,δ' protons which are shifted by approximately 0.7-0.9 ppm. This resonance shift, independent of the solvent used, is due to the closeness of the pyridyl groups to the central Pz chromophore, paralleling results previously reported for the related metal-free ligand [Py₈TPyzPzH₂] and the related precursor [(CN)₂Py₂Pyz].[9] It is worth noting that a "clean" ^{1}H-NMR spectrum for a different synthesized batch of the Mg^{II} complex was also obtained in DMF-*d*₇,[6] which indicates that the Mg^{II} complex can be easily obtained in its pure form. The Zn^{II} complex [Py₈PzZn] (either formed from the Mg^{II} complex or from the unmetalated species) and the Co^{II} and Cu^{II} analogs were also obtained in pure form as indicated by C, H, N elemental analysis and ICP-PLASMA analysis of the Zn^{II}, Co^{II} and Cu^{II} derivatives. All of the bluish [Py₈PzM] compounds (Figure 1A; M = 2H^{I}, Mg^{II}(H₂O), Zn^{II}, Co^{II}, Cu^{II}) are stable in their hydrated form after exposure to air.
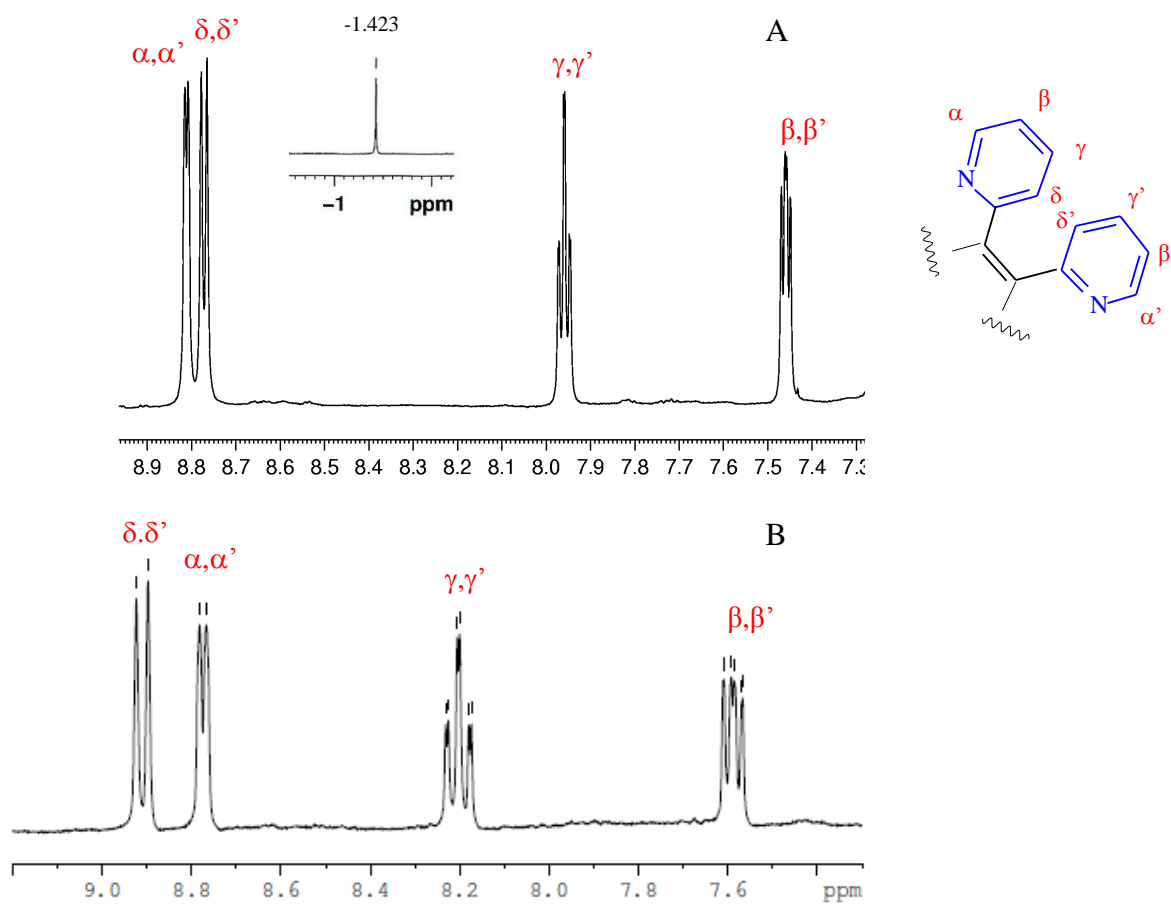
Figure 2. ^1H NMR spectra at 300 K of (A) [Py$_8$PzH$_2$] in CDCl$_3$ and (B) [Py$_8$PzMg(H$_2$O)] in DMSO-d_6. The inset shows the resonance of the protons of the central NH groups located at -1.423 ppm.

Table 1. ^1H and ^{13}C NMR Assignments for the precursor [(CN)$_2$Py$_2$Et] in DMSO-d_6, [Py$_8$PzH$_2$] in CDCl$_3$ and [Py$_8$PzMg(H$_2$O)] in DMSO-d_6 at 300 K.

	[(CN)₂Py₂Et][a]				[Py₈PzH₂]				Py₈PzMg(H₂O)			
	^1H	m	J (Hz)	^{13}C	^1H	m	J (Hz)	^{13}C	^1H	m	J (Hz)	^{13}C
								152.9[b]				154.4[b]
α,α'	8.823	ddd	4.8;1.7;1.0	150.5	8.811	d	4.8	149.5	8.775	d	4.4	150.2
β,β'	7.672	ddd	7.8;4.8;1.0	127.1	7.460	ddd	7.7; 4.8;1.0	122.7	7.590	ddd	6.9;5.6;1.0	123.7
γ,γ'	8.124	ddd	7.8;7.8;1.7	138.8	7.959	ddd	7.7;7.7;1.8	135.6	8.203	ddd	7.8;7.7;1.7	136.7
δ,δ'	8.045	ddd	7.8;1.0;1.0	125.1	8.771	d	7.7	129.0	8.910	d	7.8	129.7
NH					-1.423	s						

[a]See ref. 6.
[b]Signal of the quaternary carbon of the pyridine rings; the other signals are not visible because comparable to the background noise.

The presence of clathrated water molecules in [Py$_8$PzM] parallels previous findings for porphyrazine macrocycles bearing externally annulated heterocyclic rings.[5a] The amount of clathrated water, which can change for the different prepared batches of each species, is generally removed by mild heating (ca. 100 °C) under vacuum (10^{-2} mmHg). After the loss of water, thermogravimetric analysis of the Mg^{II} derivative indicated that the complex was stable under an inert atmosphere up to temperatures of ca. 300 °C. A comparable thermal stability was also observed for the other reported mononuclear species but exposure of the heated samples to air generally led to rehydration of the materials. Due to the limited influence of clathrated water molecules on the general physicochemical properties of the examined compounds, they will be neglected in the given formulae of the described species.

The Mg^{II} complex was earlier formulated as [Py$_8$PzMg(H$_2$O)][6] and is reported in this study as having one water molecule axially ligated to the Mg^{II} ion, in line with a similar formulation for the pyrazinoporphyrazine complex [Py$_8$PyzPzMg(H$_2$O)].[5a] The presence of such a water molecule is difficult to prove directly, but its presence is strongly suggested by the fact that the Mg(H$_2$O) moiety,

as established by crystallographic work, is commonly observed in porphyrazine and phthalocyanine macrocycles carrying central Mg^{II} ions. Examples of this are given by the complex $[(omtp)Mg(H_2O)]$[10] (omtp = octakis(methylthio)porphyrazinato dianion), a porphyrazine macrocycle carrying externally pyrrole and pyridylmethylamino groups,[11] a dimerized monohydrate of a low-symmetry porphyrazine macrocycle,[12] the phthalocyanine complexes $[PcMg(H_2O)]\cdot 2py$[13] (Pc = phthalocyaninato dianion, $C_{32}H_{16}N_8^{2-}$) and $[PcMg(H_2O)_2]$ bearing two axially ligated water molecules.[14] The presence of axially bound H_2O on Mg^{II} was also indicated for previously characterized complexes of tetrakis(thia/selenodiazole)porphyrazines.[15]

The IR spectra of $[Py_8PzH_2]$ and its Mg^{II} metal derivative over the range of 1800-600 cm^{-1} are shown in Figure 3. The Co^{II}, Cu^{II}, and Zn^{II} complexes exhibit quite similar spectral patterns. The IR spectrum of each M^{II} derivative shows a characteristic doublet in the region 900-700 cm^{-1}, which suggests a structural analogy in the series with different metal derivatives. The position of this doublet varies with changes of the central metal ion and is located at 881/835 cm^{-1} for the Mg^{II} complex (Figure 3A), 879/833 for M = Zn^{II}, 898/845 for M = Co^{II} and 892/838 for M = Cu^{II}. In contrast, $[Py_8PzH_2]$ has only a single peak at 860 cm^{-1} in the same spectral region (Figure 3B). Differences between spectra of $[Py_8PzM]$, and $[Py_8PzH_2]$ also appear in the region 1200-900 cm^{-1}. In this spectral region, $[Py_8PzH_2]$ shows a peak at 1120 cm^{-1} which is absent in spectra of the metal complexes. Finally, an intense double peak present at 998/976 cm^{-1} for $[Py_8PzH_2]$, is slightly shifted to 1006/983 cm^{-1}, 1014/985 cm^{-1}, 1010/985 cm^{-1} and 1004/982, for the Mg^{II}, Co^{II}, Cu^{II} and Zn^{II} species, respectively. This doublet can be assigned to the macrocyclic framework, its position being only slightly influenced by the specific central metal ion. In keeping with these results, worth of mention here is that the IR spectra of octaphenyl substituted porphyrazine analogs contain similar metal sensitive bands (double band near 1000 cm^{-1} and strong band at ~1150 cm^{-1}) which were assigned to CC and CN skeleton vibrations of the porphyrazine macrocycle.[IC, ICA] Noteworthy, a new absorption for $[Py_8PzH_2]$ is found at 3293 cm^{-1} (Figure 3B, inset) and is assigned as $\nu_{(NH)}$. As expected, this band disappears during formation of the M^{II} complexes (M = Co^{II}, Cu^{II}, Zn^{II}) in the process $[Py_8PzH_2] \rightarrow [Py_8PzM]$. These IR spectral features recall those observed for octaphenyl porphyrazine analogs.[16]

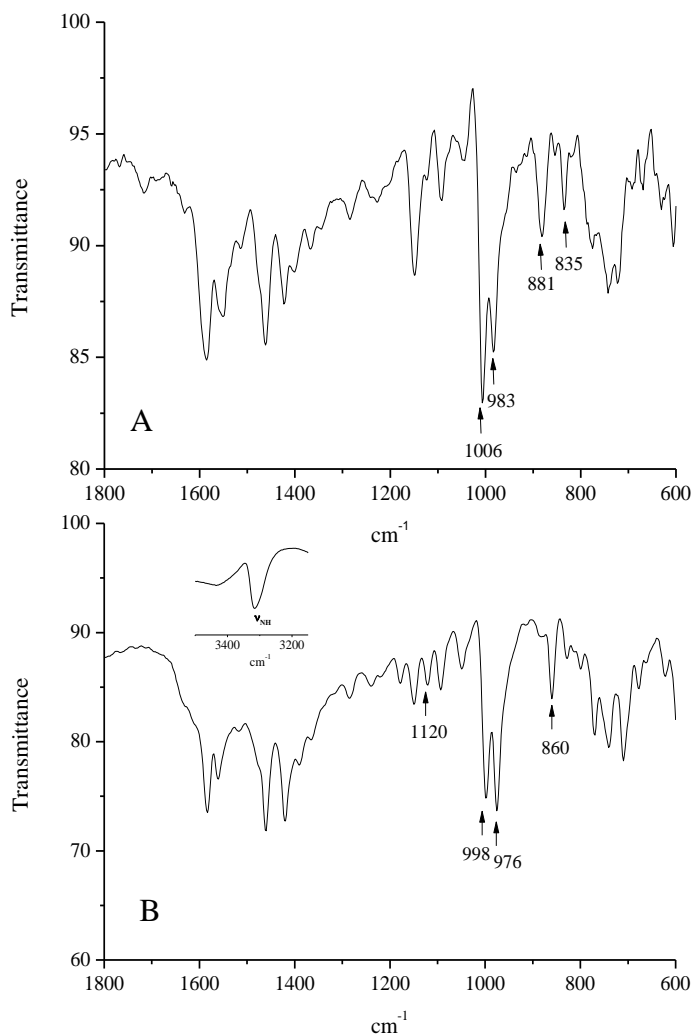**Figure 3**. IR spectra in KBr of A) [Py$_8$PzMg(H$_2$O)], B) [Py$_8$PzH$_2$] and B) [Py$_8$PzZn].

UV-Visible Spectral Behavior of [Py$_8$PzH$_2$] and the Metal Complexes [Py$_8$PzM] (Mg^{II}(H$_2$O), Co^{II}, Cu^{II}, Zn^{II}).

The examined [Py$_8$PzH$_2$] and its metal derivatives [Py$_8$PzM] possess good solubility in the polar non aqueous solvents pyridine, DMSO and DMF (c $\leq 10^{-3}$ M), and, as expected, higher than that of the related pyrazinoporphyrazine macrocycles [Py$_8$TPyzPzM]. Solubility of the [Py$_8$PzM] compounds was generally found to be lower in the non-donor solvents CHCl$_3$, CH$_2$Cl$_2$, exceptions being observed in the

case of $[Py_8PzH_2]$ and its Mg^{II} complex, for which solubility approached that observed in the low donor solvents. All of the examined compounds were stable in solution, as indicated by unchanged UV-visible spectra over a period of 24/48 h.

[Py₈PzH₂]. The spectrum of unmetalated macrocycle $[Py_8PzH_2]$ is stable with time in solutions of $CHCl_3$ and is characterized by an intense absorption in the Soret region (370 nm) and a split Q band with peaks at 594 and 663 nm (Figure 4). This type of spectrum is as expected for D_{2h} symmetry and supports the presence of the macrocycle being in its monomeric form with two central N-H groups. A low intensity peak at 637 nm can be assigned to the presence of a small amount of the dianion $[Py_8Pz]^{2-}$ in equilibrium with the neutral form. Quite similar spectra were observed in CH_2Cl_2 (peaks at 594 and 662 nm) and pyridine (peaks at 598 and 664 nm) (data listed in Table 2). The two distinct absorptions in the Q-band region are assigned as the two components of the Q band, ie. Q_x and Q_y, due to the transitions $a_u \rightarrow b_{2g}$ and $a_u \rightarrow b_{3g}$, respectively. The presence of a stable split Q band for $[Py_8PzH_2]$ at room temperature suggests a higher stability in its neutral form with respect to the related dianion $[Py_8Pz]^{2-}$ in $CHCl_3$, CH_2Cl_2 or in pyridine. The absorption in the Soret region at 370-375 nm is assigned as the B band in all the solvents, DMSO and DMF included (Table 2).

Table 2. UV-visible Spectral Data (λ, nm (log ε)) of [Py$_8$PzH$_2$] and [Py$_8$PzM] (M = Mg^{II}(H$_2$O), Co^{II}, Cu^{II}, Zn^{II}) in Different Solvents.

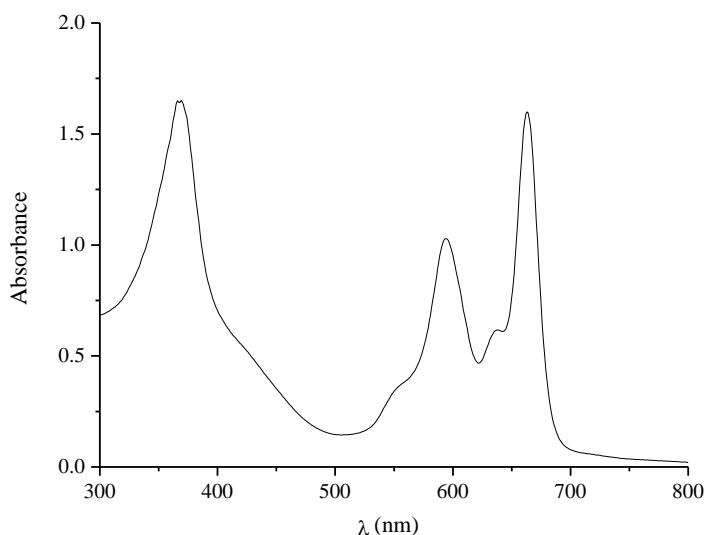| Compound	Solvent	Soret region	Q-band region		
[Py$_8$PzH$_2$]	DMF	370 (4.68)	551sh (4.04)	596 (4.45)	635 (4.46) 660 (4.64)
	DMSO	368 (4.67)	554sh (4.10)	598 (4.47)	633 (4.43) 661 (4.63)
	Py	375 (4.73)	557sh (4.11)	598 (4.53)	637 (4.36) 664 (4.71)
	CHCl$_3$	370 (4.87)	551sh (4.20)	594 (4.67)	637 (4.45) 663 (4.86)
	CH$_2$Cl$_2$	367 (4.67)	559sh (4.05)	594 (4.46)	637 (4.20) 662 (4.65)
[Py$_8$PzMg(H$_2$O)][a]	DMF	378 (5.05)	583 (4.46)		636 (5.18)
	DMSO	378 (4.52)	583 (3.95)		636 (4.63)
	py	381 (4.80)	583 (4.18)		638 (4.89)
	CHCl$_3$	378 (4.74)	583 (4.10)		637 (4.80)
[Py$_8$PzCo]	DMF	354 (4.52)	573sh (4.17)		613 (4.55)
	DMSO	357 (4.40)	572sh (3.06)		611 (4.50)
	py	356 (4.23)	571sh (3.88)		613 (4.29)
[Py$_8$PzCu]	DMF	371 (4.06)	578sh (3.62)		623 (4.24)
	DMSO	374 (4.54)	580sh (4.17)		627 (4.70)
	py	376 (4.71)	573 (4.27)		627 (5.01)
[Py$_8$PzZn]	DMF	380 (4.82)	585 (4.26)		637 (4.98)
	DMSO	380 (4.92)	584 (4.35)		636 (5.07)
	py	381 (4.85)	583 (4.27)		637 (4.97)

[a] See reference 6.

Figure 4. UV-visible spectrum of [Py$_8$PzH$_2$] in CHCl$_3$ solution.

It should be pointed out that the spectrum of the corresponding tetrapyrazinoporphyrazine compound [Py$_8$TPyzPzH$_2$], exhibits an unsplit Q band (667 nm) in pyridine.[9] This suggests a loss of the central protons and formation of the deprotonated dianion [Py$_8$TPyzPz]$^{2-}$ (D_{4h} symmetry). This result in pyridine solutions indicates that [Py$_8$TPyzPzH$_2$] is more acidic than [Py$_8$PzH$_2$]. An explanation for this result most likely resides in the fact that the pyrazine rings in the pyrazinoporphyrazine complex enhance the electron-deficiency of the macrocycle due to their electron-withdrawing properties, thus facilitating release of the central protons. A somewhat related spectral evolution was also observed for the octaphenyl substituted porphyrazine in pyridine solution.[17]

It should be noted that the observed 68-69 nm splitting of the Q bands for [Py$_8$PzH$_2$] in CHCl$_3$ and CH$_2$Cl$_2$ is much higher than the 33 nm splitting observed in the same solvents for the corresponding free-base pyrazinoporphyrazine, [Py$_8$TPyzPzH$_2$].[9] This seems to indicate that in going from [Py$_8$PzH$_2$] to [Py$_8$TPyzPzH$_2$], the splitting of the b$_{2g}$ and b$_{3g}$ HOMO energy levels decreases along with an extension of the π-delocalized system.

The examined spectral behavior of [Py$_8$PzH$_2$] in DMSO and DMF provides additional useful information about conversion of the neutral species to the corresponding dianion [Py$_8$Pz]$^{2-}$ in these solvents. Figure 5 shows the spectral changes observed for [Py$_8$PzH$_2$] in DMSO as a function of time,

combined with heating of the solution (a parallel time dependent behavior is observed in DMF). As can be seen from the figure, the initial spectrum shows two peaks at 598 and 661 nm which are attributable to the split Q_x and Q_y absorptions in addition to a peak at 633 nm, a position coincident with that of the low intensity peak also seen in the spectrum recorded in $CHCl_3$, CH_2Cl_2 and pyridine. This is clearly attributable to the presence of a small amount of the free-base macrocycle being in its dianionic $[Py_8Pz]^{2-}$ form (single Q band and D_{4h} symmetry). The combined double action of time and heating of the solution leads to an increase in intensity of the band at 633 nm and a concomitant decrease in intensity of peaks at 598 and 661 nm which are assigned to the neutral form of the compound. The final spectrum obtained after four days reveals exclusively the presence of the dianion (see Figure 6, red line). Noteworthy, differences do exist, as compared to the corresponding free-base pyrazinoporphyrazine $[Py_8TPyzPzH_2]$, which behaves the same in DMSO, DMF and pyridine solutions, giving rise immediately after dissolution to formation of the deprotonated species $[Py_8TPyzPz]^{2-}$.[9]
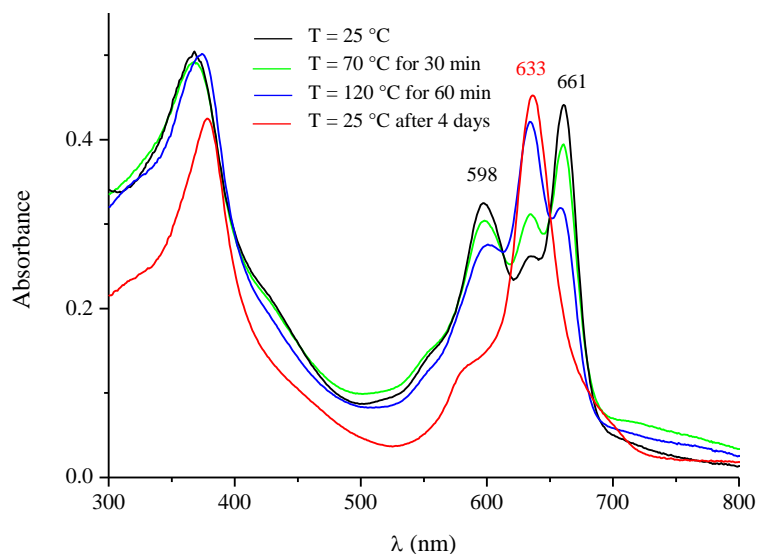

Figure 5. UV-visible spectral changes for $[Py_8PzH_2]$ in DMSO as a function of time and heating of the solution.

In order to further support the formation of the dianion $[Py_8Pz]^{2-}$ in DMSO, a titration of $[Py_8PzH_2]$ was performed in this solvent with TBAOH. The observed UV-visible spectral changes are illustrated

in Figure 6, where it can be seen that the spectrum of the neutral species changes towards that of the corresponding dianion, with the peak of this latter centered at 641 nm, only slightly batochromically shifted with respect to the position indicated in Figure 5. Accordingly, the concomitant disappearance of the absorptions of the neutral species at 597 and 661 nm is observed.
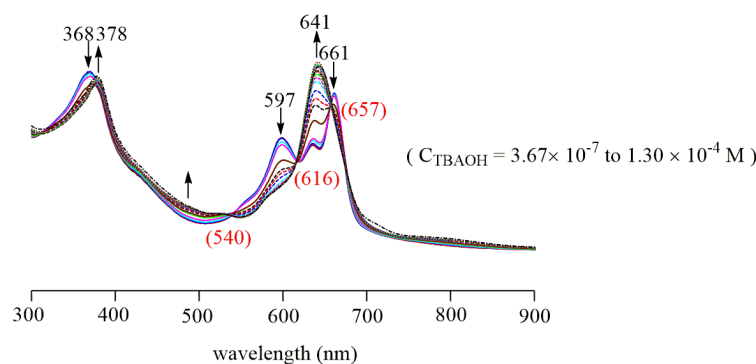

Figure 6. UV-visible spectral changes during the titration of Py_8PzH_2 with TBAOH in DMSO.

Spectral behaviour of the complexes [Py₈PzM] (Mg^{II}(H₂O), Co^{II}, Cu^{II}, Zn^{II}). The UV-visible spectra of the metal complexes in pyridine, DMSO and DMF all show similar well-defined profiles (see example in Figure 7), with a single band in the Soret region of the spectrum (340-450 nm) and sharp unsplit Q bands in the region 610-640 nm which are attributable to ligand-centered $\pi \to \pi^*$ transitions in an approximate D_{4h} symmetry. The overall shape of the spectra indicate the presence of the almost exclusively monomeric species, even at the highest examined concentrations (ca. 10^{-3} M in DMF). The observed spectral features suggest a behavior which is in line with previous findings for M^{II} pyrazinoporphyrazines.[18]

Quantitative spectral data for the [Py₈PzM] complexes (M = $Mg^{II}(H_2O)$, Co^{II}, Cu^{II}, Zn^{II}) are summarized in Table 2. In general, the Soret and Q bands exhibit only a small solvent effect, analogous to what is seen for the parallel series of pyrazinoporphyrazines. However, a marked change in the position of the Q-band maxima is seen with changes in the central metal ion, which increases in the sequence: Co^{II} (611-612 nm), Cu^{II} (623-627 nm), and Mg^{II} and Zn^{II} (636-638 nm). Interestingly, the same sequence of shifts occurs for the pyrazinoporphyrazine analogs: Co^{II} (634-635 nm), Cu^{II} (648-653 nm), and Mg^{II} and Zn^{II} (653-658 nm).[5a,b] From these data it clearly appears that moving from the

[Py$_8$PzM] complexes to the corresponding pyrazinoporphyrazines [Py$_8$TPyzPzM] results in a 20-25 nm bathochromic shift of the Q-band maxima for each metal derivative. This bathochromic shift is determined by the increased extension of the π-electron delocalization consequent to incorporation of the pyrazine rings in going from [Py$_8$PzM] to [Py$_8$TPyzPzM]. This behavior is reminiscent of similar findings for other porphyrazines, phthalocyanines and naphtahlocyanines.[19] A rational explanation of the observed spectral behavior was earlier provided by TDDFT calculations for [Py$_8$PzMg], [Py$_8$TPyzPzMg] and [Py$_8$QxPzMg] which are water-free model compounds of the corresponding axially-hydrated triad [Py$_8$PzMg(H$_2$O)], [Py$_8$TPyzPzMg(H$_2$O)] and [Py$_8$QxPzMg(H$_2$O)] (Qx = quinoxaline; see Figure 1). The theoretical calculations agree well with the UV-visible experimental data[6] in that there is a shift of the Q-band maxima from 636 to 658 and then to 759 nm in DMF as the macrocycle π-system is further increased.

Figure 7. UV-visible spectra of the complexes [Py$_8$PzM] (M = Mg^{II}(H$_2$O), Co^{II}, Cu^{II}, Zn^{II}) in DMF.

Electrochemistry

[Py$_8$PzH$_2$] and the triad of complexes [Py$_8$PzM] (M = Mg^{II}(H$_2$O), Zn^{II}, Cu^{II}) were electrochemically investigated in DMSO and pyridine, while [Py$_8$PzCo] was investigated in the same two solvents in addition to PhCN and CH$_2$Cl$_2$. Previous electrochemical studies on the related pyrazinoporphyrazine

macrocycles derivatives $[Py_8TPyzPzH_2]$[9]and $[Py_8TPyzPzM]$,[5a,b,d,2d] and similar macrocycles bearing annulated diazepine[20] and thienyl rings,[21] have generally shown that each porphyrazine macrocyclic species can be reduced in four one-electron transfer steps and this is also the case for the currently investigated compounds, although the current-voltage curves were in many cases "complicated" by the presence of aggregation under some of the solution conditions. The electrochemical behavior of the present compounds is detailed here below.

$[Py_8PzH_2]$. Cyclic voltammograms of the metal-free $[Py_8PzH_2]$ in pyridine are illustrated in Figure 8. The first two reductions are reversible and involve one electron additions to the macrocycle generating $[Py_8PzH_2]^-$ and $[Py_8PzH_2]^{2-}$, respectively. These processes occur at $E_{1/2}$ = -0.26 and -0.65 V vs. SCE and can be compared to $E_{1/2}$ values of -0.17 and -0.48 V for the corresponding reductions of $[Py_8TPyzPzH_2]$ under the same solution conditions.[9] Two reversible one-electron reductions of $[Py_8PzH_2]$ are also observed in DMSO (at $E_{1/2}$ = -0.17 and -0.57 V).

A third reversible reduction of $[Py_8PzH_2]$ is observed at -0.93 V in pyridine (see Fig. 7) and this process corresponds to reduction of the deprotonated $[Py_8Pz]^{2-}$ macrocycle according to eq. 1 as described earlier for $[Py_8TPyzPzH_2]$.[9]

$$[Py_8Pz]^{2-} + e^- \rightleftharpoons [Py_8Pz]^{3-} \qquad (1)$$

The first and second reductions of $[Py_8PzH_2]$ are harder than the first and second reductions of $[Py_8TPyzPzH_2]$, which is consistent with the smaller conjugated system in $[Py_8PzH_2]$. The same order in ease of reduction is also observed for the metal derivatives of these two macrocycles as described on the following pages. Surprisingly, the measured half wave potential for reduction of the deprotonated $[Py_8Pz]^{2-}$ in pyridine is exactly the same as $E_{1/2}$ for reduction of $[Py_8TPyzPz]^{2-}$ (-0.93 V) under the same solution conditions. Almost identical values in half-wave potentials are also seen for the same two macrocycles in DMSO where $[Py_8Pz]^{2-}$ is reduced at -0.87 V and $[Py_8TPyzPz]^{2-}$ at -0.89 V (see Table 3).
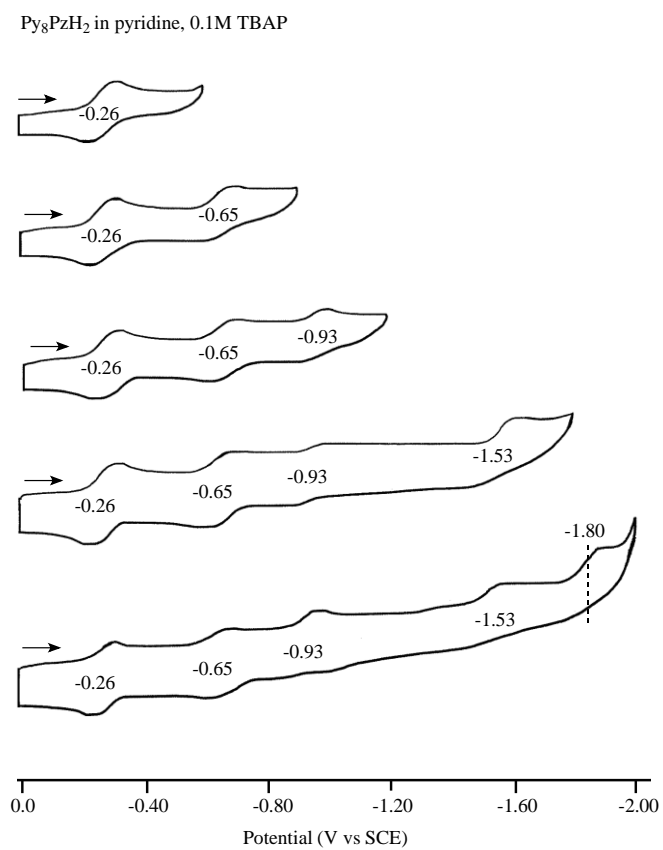
Py$_8$PzH$_2$ in pyridine, 0.1M TBAP

Figure 8. Cyclic voltammograms of [Py$_8$PzH$_2$] in pyridine, 0.1M TBAP. Scan rate = 0.1 V/s.

Table 3. Half-Wave Potentials ($E_{1/2}$, V vs SCE) of [Py$_8$PzM] and [Py$_8$PyzPzM] (M = 2H^I, Cu^{II}, Zn^{II}, Mg(H$_2$O), Co^{II}) in Py and DMSO, containing 0.1M TBAP.

Solvent	Macrocycle	Reduction					ref.
		1st	2nd	[Pz]$^{2-}$/[Pz]$^{3-}$	3rd	4th	
Py	[Py$_8$PzH$_2$]	-0.26	-0.65	-0.93	-1.53	-1.86[a]	tw.
	[Py$_8$TPyzPzH$_2$]	-0.17	-0.48	-0.93	-1.24	-1.61	9
	[Py$_8$PzCu]	-0.38					tw.
	[Py$_8$TPyzPzCu]	-0.30	-0.68		-1.28	-1.61	5a
	[Py$_8$PzZn]	-0.46	-0.91		-1.66[a]	-1.92[a]	tw.
	[Py$_8$TPyzPzZn]	-0.34	-0.72		-1.38	-1.66	5a
	[Py$_8$Pz Mg(H$_2$O)]	-0.54	-0.93		-1.49	-1.84[a]	tw.
	[Py$_8$TPyzPz Mg(H$_2$O)]	-0.40	-0.79		-1.43	-1.70	5a
	[Py$_8$PzCo]	-0.33	-1.01		-1.60	-1.92[a]	tw.
	[Py$_8$TPyzPzCo]	-0.26	-0.87		-1.37	-1.83	5a
DMSO	[Py$_8$PzH$_2$]	-0.17	-0.57	-0.87	-1.44	-1.80[a]	tw.
	[Py$_8$TPyzPzH$_2$][b]	-0.16	-0.40	-0.89	-1.21	-1.57	5b
	[Py$_8$PzCu]	-0.34	-0.67				tw.
	[Py$_8$TPyzPzCu]	-0.33	-0.58		-1.22	-1.58	5b
	[Py$_8$PzZn]	-0.43	-0.85		-1.57	-1.88	tw.
	[Py$_8$TPyzPzZn]	-0.26	-0.67		-1.38	-1.64	5b
	[Py$_8$PzMg(H$_2$O)]	-0.44					tw.
	[Py$_8$TPyzPzMg(H$_2$O)]	-0.33	-0.70		-1.39	-1.67	5b
	[Py$_8$PzCo]	-0.19	-0.95		-1.53	-1.85	tw.
	[Py$_8$TPyzPzCo]	-0.06	-0.76		-1.31	-1.77	5b

[a] Irreversible reduction reaction at scan rate = 100 mV/s.

 tw. = this work.

The last two reductions of [Py$_8$PzH$_2$] in pyridine are located at $E_{1/2}$ = -1.53 V and E_{pc} = -1.86 V as seen in Figure 8. Like the first two reductions, these processes are harder (occur at more negative potentials) than the third and fourth reductions of [Py$_8$TPyzPzH$_2$] in the same solvent, the magnitude of the potential difference between the relevant redox reactions being 290 and ~250 mV, respectively (see Table 3). The lack of well-defined reoxidation peaks for the reductions of [Py$_8$PzH$_2$] at -1.53 and -1.86

V are most likely related to equilibria involving the fully protonated porphyrazines and the deprotonated porphyrazine in its initial and/or singly reduced form, i.e. $[Py_8Pz]^{2-}$ and $[Py_8Pz]^{3-}$.

$[Py_8PzM]$ where $M = Cu^{II}$, Zn^{II} and $Mg^{II}(H_2O)$. The first one-electron reduction of the Cu^{II}, Zn^{II} and $Mg^{II}(H_2O)$ porphyrazines is well defined in pyridine and located at -0.38, -0.46 and -0.54 V, respectively. These values can be compared to the first one-electron reduction of the analogous $[Py_8TPyzPzM]$ derivatives which are reduced at -0.30, -0.34 and -0.40 V, respectively as seen in Table 3. Thus, like in the case of the free-base derivatives, more facile reductions are again seen for $[Py_8TPyzPzM]$ than for $[Py_8PzM]$, with the exact difference in potential varying with the type of central metal ion and following the order: Cu^{II} ($\Delta E_{1/2} = 80$ mV) $< Zn^{II}$ ($\Delta E_{1/2} = 120$ mV) $< Mg^{II}(H_2O)$ ($\Delta E_{1/2} = 140$ mV). The above separation in $E_{1/2}$ between the two related metallomacrocycles with the same metal ion can be compared with a $\Delta E_{1/2}$ of 90 mV between half-wave potentials for the first reduction of $[Py_8PzH_2]$ and the first reduction of $[Py_8TPyzPzH_2]$ (see above discussion and Table 3).

A second reversible one-electron reduction of $[Py_8PzZn]$ is observed in pyridine and DMSO. These reductions occur at -0.91 and -0.85 V, respectively, and are shifted negatively by 180 to 190 mV from $E_{1/2}$ values of $[Py_8TPyzPzZn]$ in the same solutions, thus suggesting that the effect of the different π systems on $E_{1/2}$ values is greater for the second electron addition than for the first.

Unfortunately, all other electroreductions of the Cu^{II}, Zn^{II} and $Mg^{II}(H_2O)$ porphyrazines are ill-defined due to the presence of aggregation after electroreductions. This is seen by the cyclic voltammograms in Figure 9.
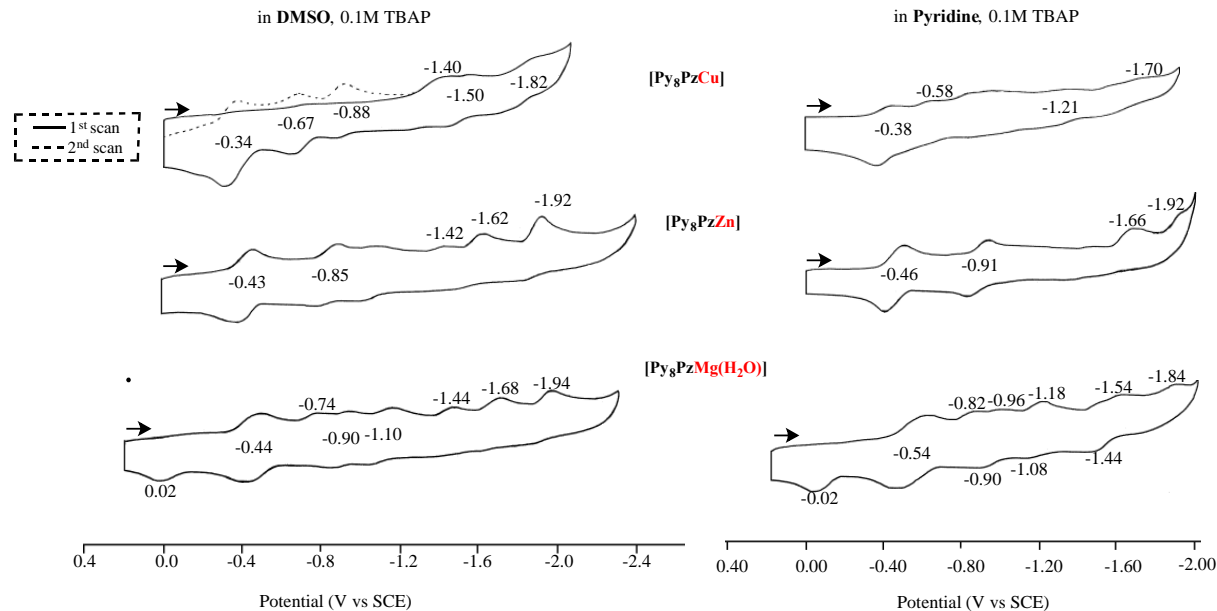
Figure 9. Cyclic voltammograms of [Py$_8$PzM] with M = Cu^{II}, Zn^{II} and Mg^{II}(H$_2$O), in DMSO and Pyridine, 0.1M TBAP. Scan rate = 0.1 V/s.

[Py$_8$PzCo^{II}]. The Co^{II} complex is characterized by four one-electron reductions in pyridine and five in DMSO. A single oxidation is also observed at +0.25 V in pyridine. This process is quasi-reversible and corresponds to the reaction Co^{II}/Co^{III}. A similar Co^{II}/Co^{III} process has been reported for the pyrazinoporphyrazine complex [Py$_8$TPyzPzCo] in DMSO[5b] as well as for Co^{II}-phthalocyanines.[22]

The first one-electron reduction of [Py$_8$TPyzPzCo] to its Co^{I} form is reversible in DMSO[5b] and this is also true for cobalt phthalocyanine [PcCo^{II}] in this solvent. Both of these processes occur at similar half wave potentials of -0.06 and -0.08 V (data in Figure 10), but this is not the case for [Py$_8$PzCo] where the reduction and reoxidation reactions are split into two separate processes which are located at E_{pc} = -0.32 V and E_{pa} = -0.06 V for a scan rate of -0.1 V/s (see Figure 10).

in DMSO, 0.1M TBAP
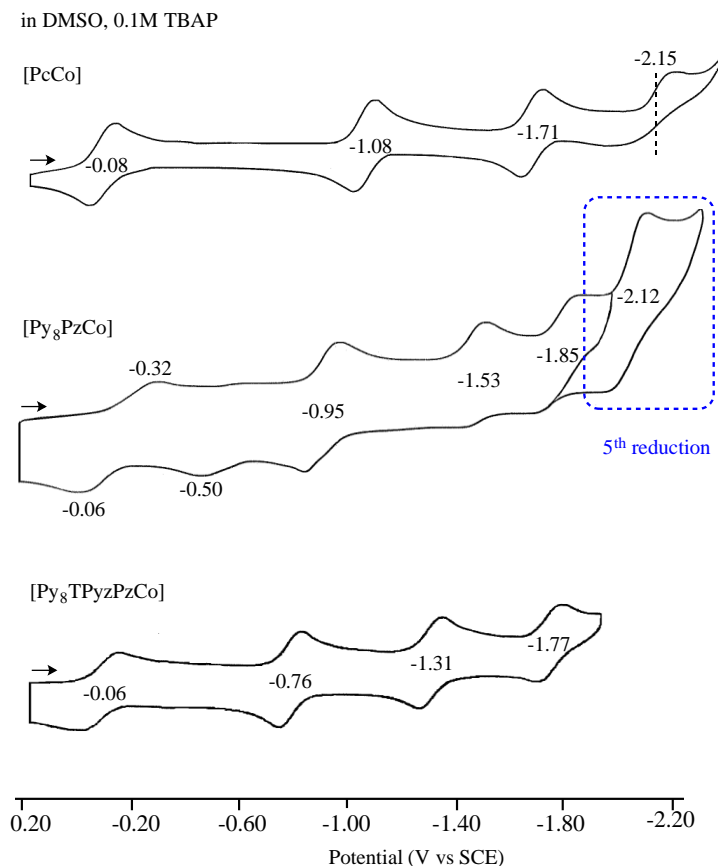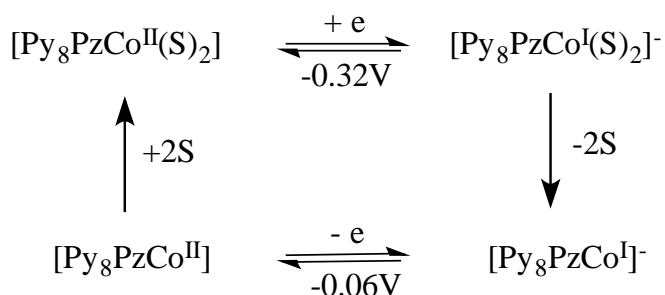
[PcCo]

-2.15

-1.71

-1.08

-0.08

[Py$_8$PzCo]

-2.12

-1.85

-1.53

-0.95

-0.32

-0.50

-0.06

5th reduction

[Py$_8$TPyzPzCo]

-1.77

-1.31

-0.76

-0.06

| 0.20 | -0.20 | -0.60 | -1.00 | -1.40 | -1.80 | -2.20 |

Potential (V vs SCE)

Figure 10. Cyclic voltammograms for [PcCo], [Py$_8$PzCo] and [Py$_8$TPyzPzCo] in DMSO, 0.1M TBAP. Scan rate = 0.1 V/s

This large separation of reduction and oxidation peaks for the Co^{II}/Co^{I} and reverse Co^{I}/Co^{II} reaction of [Py$_8$PzCo] can be accounted for by a well-known box mechanism[23] of the type illustrated in Scheme 1. The reduction at E_{pc} = -0.32 V involves electron addition to a six coordinate Co^{II} porphyrazine while the reoxidation at E_{pa} = -0.06 V involves electron abstraction from an unsolvated four-coordinate Co^{I} form of the compound.

$$[Py_8PzCo^{II}(S)_2] \quad \xrightleftharpoons[-0.32V]{+ e} \quad [Py_8PzCo^{I}(S)_2]^-$$

$$\uparrow +2S \qquad\qquad\qquad -2S \downarrow$$

$$[Py_8PzCo^{II}] \quad \xrightleftharpoons[-0.06V]{- e} \quad [Py_8PzCo^{I}]^-$$

Scheme 1. Mechanism for the reduction and reoxidation of [Py$_8$PzCo] in DMSO, 0.1M TBAP.

24

The almost identical $E_{1/2}$ values for the first reduction of [PcCo] (-0.08 V) and [Py$_8$TPyzPzCo] (-0.06 V) indicates a negligible difference in how these two macrocycles effect the Co^{II}/Co^I process of the compounds. However, this is not the case for the second, third and fourth reductions of the three related species, where the ease of electron addition follows the order: [Py$_8$TPyzPzCo] > [Py$_8$PzCo] > [PcCo] for each redox process beyond the first. The absolute difference between the measured reduction potential of [Py$_8$PzCo] and [Py$_8$TPyzPzCo] amounts to 190 mV for the second electron addition, 210 mV for the third and 80 mV for the fourth. A fifth, never before seen reduction of [Py$_8$PzCo] is also present in DMSO and this may be related to the fact that four ring-centered reductions and one metal-centered Co^{II}/Co^I process are expected to occur for this compound.

In this regard, it should be pointed out that the reversible third and fourth reductions of [Py$_8$TPyzPzCo] were earlier proposed to generate a Co^{II} porphyrazine with a triply and quadruply reduced macrocycle[5b] and this may also be the case for [Py$_8$PzCo] where $E_{1/2}$ values for addition of the third and fourth electrons are quite similar to measured potentials for reduction of the [Py$_8$PzZn] derivative under similar solution conditions (see Table 3).

Finally, the axial coordination of pyridine to the Co^{III} and Co^{II} forms of [Py$_8$PzCo] in CH$_2$Cl$_2$ and neat pyridine was investigated. Aggregation of [Py$_8$PzCo] is present in CH$_2$Cl$_2$ solutions and, under these conditions, neither the first metal-centered reduction nor first metal-centered oxidation can be observed in initial scans by cyclic voltammetry. However, the extent of aggregation decreases upon addition of pyridine to solution and in CH$_2$Cl$_2$/pyridine mixtures, three well-defined reductions and one oxidation can be easily detected. The potentials for the second and third reductions are almost invariant with changes in the CH$_2$Cl$_2$/pyridine ratio but this is not the case for the first oxidation and first reduction where the half-wave potentials vary systematically with the concentration of pyridine as shown by the data in Figure 11.

The measured $E_{1/2}$ for the Co^{II}/Co^{III} and Co^{II}/Co^{I} processes of [Py$_8$PzCo] initally shifts by 53-59 mV per ten-fold change in the log[py] concentration (Region I of Figure) but as more pyridine is added to solution, the half-wave potentials for these two reactions stop shifting, as shown in Region I of the figure. The magnitude of the shift follows classical behavior for the loss or gain of axial ligands upon oxidation or reduction[23] and the overall mechanism for the first electron addition and first electron abstraction of [Py$_8$PzCo] is as described in the figure. In CH$_2$Cl$_2$ solutions with low concentrations of pyridine, the prevailing electrode reactions involve [Py$_8$PzCo^{III}(Py)$_2$]$^+$, [Py$_8$PzCo^{II}(Py)] and [Py$_8$PzCo^{I}]$^-$ species, while in solutions with higher concentrations the reactive species are all six-coordinate on the timescale of the electron transfer, i.e. [Py$_8$PzCo^{III}(Py)$_2$]$^+$, [Py$_8$PzCo^{II}(Py)$_2$] and [Py$_8$PzCo^{I}(Py)$_2$]$^-$.

REGION I   REGION II

0.36

1st oxidation

0.32

0.28

$E_{1/2}$ (V)

0.24

Slope = -59.0 mV

Slope = 0.0 mV

0.2

-0.16

1st reduction

-0.2

$E_{1/2}$ (V)

-0.24

Slope = -53.0 mV   Slope = 0.0 mV

-0.28

-0.32

-3   -2   -1   0

log[pyridine]

REGION I   REGION II

$[(Py)_8PzCo^{III}(S)_2]^+ + e \rightleftharpoons [(Py)_8PzCo^{II}(S)] + S$ $[(Py)_8PzCo^{III}(S)_2]^+ + e \rightleftharpoons [(Py)_8PzCo^{II}(S)_2]$

$[(Py)_8PzCo^{II}(S)] + e \rightleftharpoons [(Py)_8PzCo^I]^- + S$ $[(Py)_8PzCo^{II}(S)_2] + e \rightleftharpoons [(Py)_8PzCo^{II}(S)_2]^{2-}$

Where S = pyridine

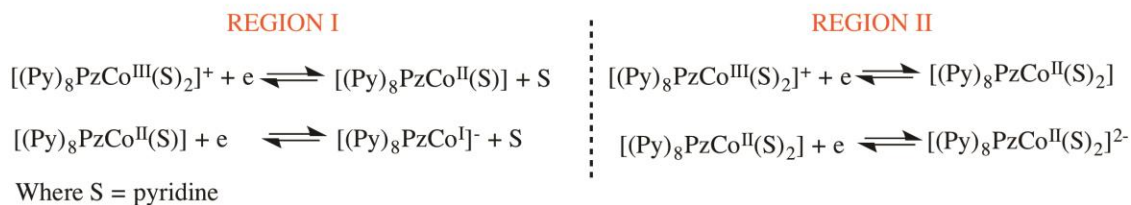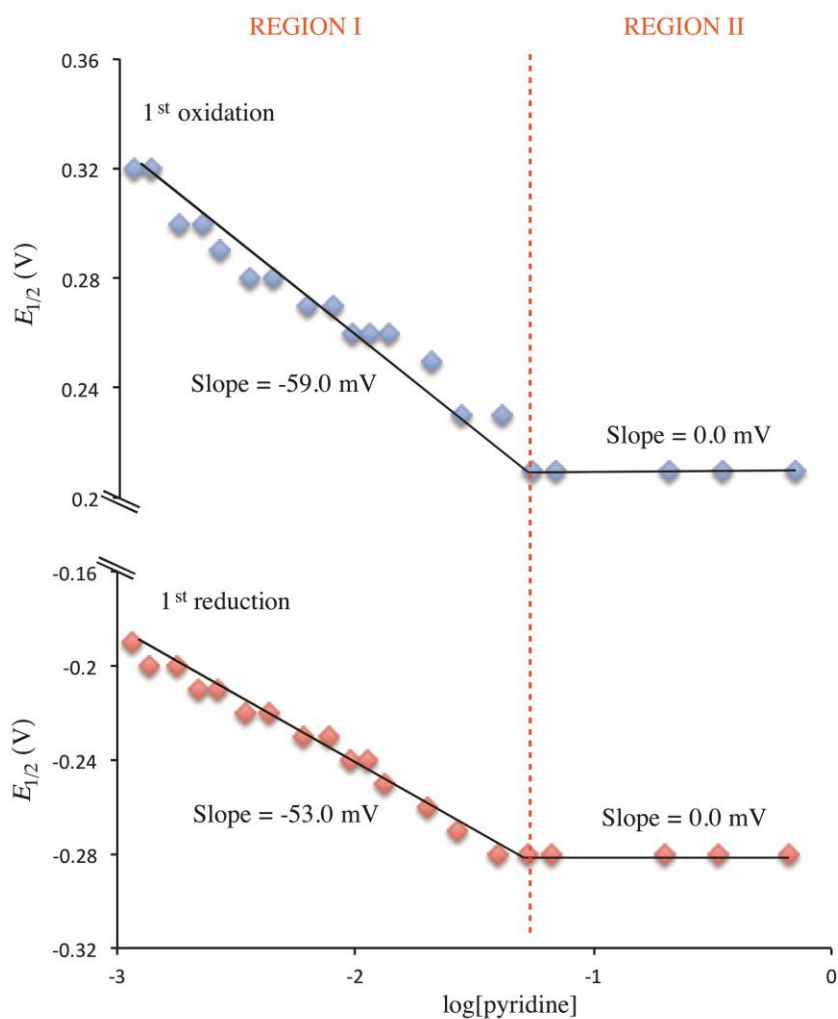**Figure 11**. Plot of $E_{1/2}$ for the first oxidation and first reduction of [Py$_8$PzCo] in CH$_2$Cl$_2$ vs log of the pyridine concentration added to solution.

Quantum Yields of Singlet Oxygen (Φ_Δ) and Fluorescence (Φ_F) of [Py$_8$PzM] in DMF.

The efficiency of singlet oxygen production, expressed by the singlet oxygen quantum yield Φ_Δ values, of the complexes [Py$_8$PzM] (M = Mg^{II}(H$_2$O), Zn^{II}), were examined in DMF and the results are presented in Table 4. The measurements were performed by an absolute method, using a laser source at 635 nm, which is close to the Q-band absorption peaks for the two complexes. Solutions were found to be stable under laser irradiation during the experiments (Figure 12A). A drawing exemplifying a typical Stern-Volmer plot used to calculate the singlet oxygen quantum yield (Φ_Δ) of the sensitizers, according to Eq. 1 (see Experimental Section), is shown in Figure 12B for [Py$_8$PzZn]. The first inset illustrates the related experimental data corresponding to the absorption decay at 414 nm for the ^{1}O$_2$ scavenger, DPBF, recorded during irradiation of the solution. The Φ_Δ values are reported in Table 4 (see Experimental Section for the k_d/k_r values). Fluorescence quantum yields (Φ_F) obtained in DMF for the same species (c $\leq$ 10^{-6} M) are also listed in the table.
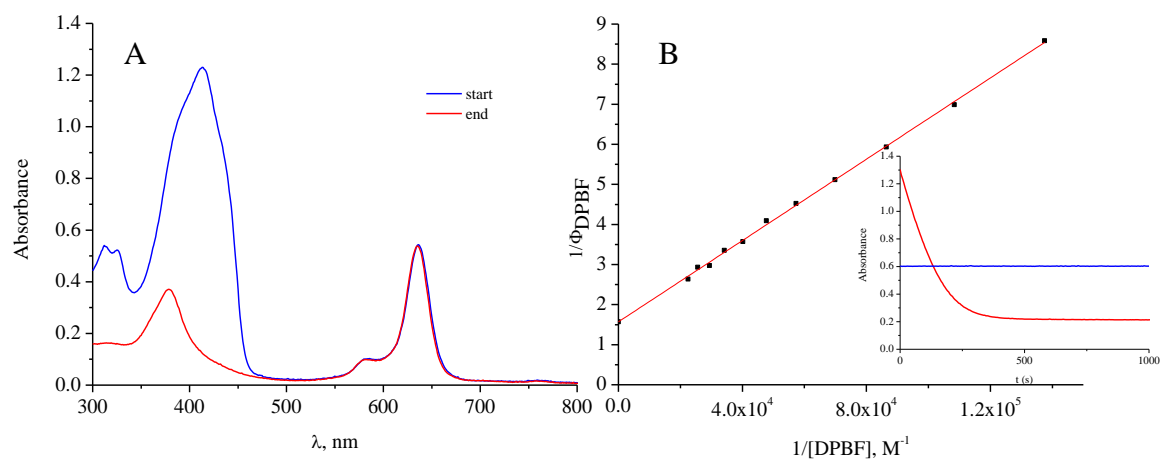

Figure 12 A: UV-visible Spectra in DMF solution of [Py$_8$PzZn] and DPBF before (blue line) and after (red line) laser irradiation (λ_{irr} = 635 nm); B: Stern-Volmer data analysis of the DPBF photooxidation (see inset; the blue line indicates stability of the complex during irradiation).

Table 4. Singlet Oxygen (Φ_Δ) and Fluorescence Quantum Yields (Φ_F) in DMF of the species [Py$_8$PzM] (M = Mg^{II}(H$_2$O), Zn^{II}).

Compound		Singlet Oxygen		Fluorescence (λ_{exc}= 600 nm)	
	λ_{max} [nm]	λ_{irr} [nm]	$\Phi_\Delta{}^a$	λ_{em} [nm]	$\Phi_F{}^a$
[Py$_8$PzMg(H$_2$O)]	636	635	0.42	650	0.25
[Py$_8$PzZn]	637	635	0.64	650	0.18

[a] Mean value of at least three measurements. Uncertainty is half dispersion and is typically ± 0.03.

As can be seen in Table 4, the observed Φ_Δ values for the Zn^{II} and Mg^{II} complexes follow the order Zn^{II} > Mg^{II}, due to the "heavy atom effect" which enhances the triplet excited state quantum yield for Zn^{II} with respect to Mg^{II}. Indeed, the introduction of a heavier metal ion into a porphyrazine macrocycle increases the rate of intersystem crossing via enhancement of *spin-orbit coupling*, favoring formation of a triple T$_1$ state with an adequate energy and lifetime to allow for proper energy transfer to dioxygen for the process $^3O_2 \rightarrow {}^1O_2$ to occur.

The measured Φ_Δ values for the Zn^{II} (0.64) and the Mg^{II} (0.42) compounds fall within the range of values reported in the literature for neutral Zn^{II} and Mg^{II} phtalocyanine and porphyrazine derivatives (0.4-0.6 for Zn^{II}; 0.2-0.4 for Mg^{II})[24-28] indicating that both species exhibit a promising response for applications in PDT. A comparison of the Φ_F values for the two metal centers also seems to be in line with expectation, i.e., the values of the Mg^{II} complexes are higher than those of the Zn^{II} analogs, which is consistent with the reverse order found for Φ_Δ.

It should be pointed out that higher Φ_Δ values have been observed for compounds with the same metal center upon going from the earlier decribed pyrazinoporphyrazines to the currently examined porphyrazines, i.e. [Py$_8$TPyzPzZn]$_{DMF}$ (0.55) $\rightarrow$ [Py$_8$PzZn]$_{DMF}$ (0.64) for the Zn^{II} complexes and [Py$_8$TPyzPzMg(H$_2$O)]$_{DMF/HCl}$ (0.29) $\rightarrow$ [Py$_8$PzMg(H$_2$O)]$_{DMF}$ (0.42) for the Mg^{II} species. This suggests that the more extended pyrazinoporphyrazine macrocycle has a higher facility to dissipate the excitation energy by nonradiative internal conversion processes, which leads to a decrease of the singlet and triplet excited state lifetimes (τ_{S1} and τ_T) and of their quantum yields (Φ_{S1}, Φ_T) with an

implied decrease of the Φ_Δ values. This behavior closely recalls the trend observed for other tetrapyrrolic macrocycles such as naphthalocyanines (Nc) and phtalocyanines (Pc), i.e. [NcZn]$_{DMF}$ (0.36) and [PcZn]$_{DMF}$ (0.49).[25a-c]

Fluorescence emission spectra typical of porphyrazine macrocycles were obtained for the Zn^{II} complex [Py$_8$PzZn]. Figure 13 shows its absorption, excitation and emission spectra. The overall coincidence of the narrow Q bands in the absorption and excitation spectra indicates that monomeric species is almost exclusively present in solution.
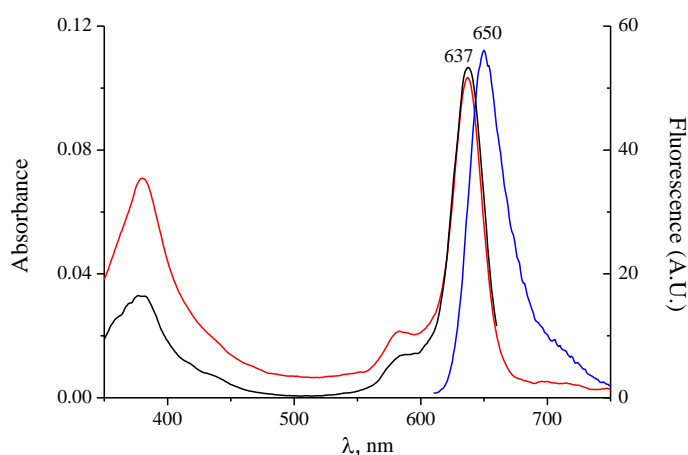

Figure 13. UV-visible absorption (red line), fluorescence excitation (black line; λ_{em} = 670 nm) and emission (blue line; λ_{exc} = 600 nm) spectra of [Py$_8$PzZn] in DMF .

Conclusions

As part of our continuing studies on porphyrazine compounds, which included extensive work conducted on the recently partly reviewed tetrapirazinoporphyrazines of formula [Py$_8$TPyzPzM] (M = bivalent metal ion), it was found of great interest to explore the effect of reducing or extending the size of the central pyrazinoporphyrazine macrocyclic framework, thus modifying the level of the π-electron delocalization. Previously octapyridinated Mg^{II} complexes were prepared of formula [Py$_8$PzMg(H$_2$O)], formally derived from the corresponding species [Py$_8$TPyzPzMg(H$_2$O)] by removing the pyrazine rings, and [Py$_8$QxPzMg(H$_2$O)] with the pyrazine rings in turn substituted by quinoxaline rings. It has been shown that the Q-band maximum for the triad of the Mg^{II} complexes moves remarkably toward

the red with the extension of the macrocyclic π-system. In the present work attention has been focused on the unmetalated macrocycle of reduced size [Py$_8$PzH$_2$] obtained by demetalation of the related Mg^{II} complex in CH$_3$COOH under mild experimental conditions. The available [Py$_8$PzH$_2$] allowed access to the formation of centrally metalated derivatives of formula [Py$_8$PzM] (M = Co^{II}, Cu^{II} and Zn^{II}) which have been the object of this research work.

UV-visible spectra of [Py$_8$PzH$_2$] in solution of non donor solvents (CH$_2$Cl$_2$, CHCl$_3$) and in pyridine are indicative of D_{2h} symmetry, as suggested by the observed large splitting of the Q band peaks (ca. 65 nm). Spectral changes in solution of DMSO and DMF show that [Py$_8$PzH$_2$] irreversibly results along with the time in the formation to its corresponding dianion [Py$_8$Pz]$^{2-}$. The overall spectral data suggest lower acidity for the smaller macrocycle [Py$_8$PzH$_2$] with respect to that of [Py$_8$TPyzPzH$_2$], the findings being in strict relationship with the different extension of the π-electron delocalized system for the two species. UV-visible spectra of the complexes [Py$_8$PzM] (M = Co^{II}, Cu^{II}, Zn^{II}), similarly to what previously reported for the Mg^{II} analog, show clean UV-visible spectral profiles in pyridine, DMSO and DMF, typical of monomeric species, with the Q band hypsochromically shifted by 20-25 nm with respect to the corresponding values of the parallel series of [Py$_8$TPyzPzM] compounds, this confirming for the two series of compounds the dependence of the UV-visible spectral behaviour by the different size of the macrocycle and level of π-electron distribution. Cyclic voltammetric studies of [Py$_8$PzH$_2$] show that the observed reversible first and second one-electron reductions in pyridine solution generating [Py$_8$PzH$_2$]$^-$ and [Py$_8$PzH$_2$]$^{2-}$ are found at more negative $E_{1/2}$ values (similar values in DMSO) than those for [Py$_8$TPyzPzH$_2$], data proving that harder reductions are occurring for [Py$_8$PzH$_2$], in keeping with its smaller π-conjugated system. The third and the fourth reductions for [Py$_8$PzH$_2$] follow the same trend. Well defined first one-electron reductions occur in pyridine for the Cu^{II}, Zn^{II} and Mg^{II} complexes at slightly more negative $E_{1/2}$ values than those of the [Py$_8$TPyzPzM] systems, paralleling the results for the unmetalated species. A second reversible one-electron reduction is observed for the Zn^{II}

complex in pyridine and DMSO, but all other reductions of the Zn^{II}, Cu^{II}, and $Mg(H_2O)$ complexes are ill defined due mainly to aggregation, among other possible reasons (demetalization?). Four one-electron nicely reversible steps of reduction are observed for the Co^{II} complex [Py_8PzCo] in pyridine (five in DMSO). The Co^{II}/Co^{III} oxidation process occurs in pyridine, recalling similar processes in DMSO for [$Py_8TPyzPzCo$] and Co^{II}-phthalocyanines. The first one-electron uptake and release for [Py_8PzCo] in DMSO has been interpreted as metal centered, ie. Co^{II}/Co^{I} and reverse Co^{I}/Co^{II} processes, involving the "box-mechanism", details of which are given in the text; this is in line with the findings for [$Py_8TPyzPzCo$] and [$PcCo$] in the same solvent, the difference being that for [Py_8PzCo] the process is split into two separate processes, characterized by E_{pc} and E_{pa} values different by 0.24 V vs SCE. Other aspects of the overall electrochemical behavior of [Py_8PzCo] have been illustrated and discussed. Finally, the measured photoactivity for the generation of singlet oxygen, $^1O_2$, of the complexes [$Py_8PzMg(H_2O)$] and [Py_8PzZn] in DMF solution has led to quantum yield values (Φ_Δ) of, respectively, 0.42 and 0.64, coherent with the "heavy atom effect", the high value for the Zn^{II} complex suggesting this latter as a highly promising material for future applications in Photodynamic Therapy (PDT).

Author Information

Corresponding Authors:

* E-mail: mariapia.donzello@uniroma1.it

* E-mail: kadish@Central.UH.EDU

References

(1) Donzello, M. P.; Ercolani, C.; Novakova, V.; Zimcik, P.; Stuzhin, P. A. Tetrapyrazinoporphyrazines and their metal derivatives. Part I: Synthesis and basic structural information. *Coord. Chem. Rev.* **2016**, *309*, 107-179.

(2) (a) Donzello, M. P.; Viola, E.; Bergami, C.; Dini, D.; Ercolani, C.; Giustini, M.; Kadish, K. M.; Meneghetti, M.; Monacelli, F.; Rosa, A. Tetra-2,3-pyrazinoporphyrazines with Externally Appended Pyridine Rings. 6. Chemical and Redox Properties and Highly Effective Photosensitizing Activity for Singlet Oxygen Production of Penta- and Monopalladated Complexes in Dimethylformamide Solution. *Inorg. Chem.* **2008,** *47*, 8757-8766. (b) Donzello, M. P.; Vittori, D.; Viola, E.; Manet, I.; Mannina, L.; Cellai, L.; Monti, S.; Ercolani, C. Tetra-2,3-pyrazinoporphyrazines with Externally Appended Pyridine Rings. 9. Novel Heterobimetallic Macrocycles and Related Hydrosoluble Hexacations as Potentially Active Photo/Chemotherapeutic Anticancer Agents. *Inorg. Chem.* **2011,** *50*, 7391-7402. (c) Donzello, M. P.; Viola, E.; Mannina, L.; Barteri, M.; Fu, Z.; Ercolani, C. Tetra-2,3-pyrazinoporphyrazines with externally appended pyridine rings. 11. Photoactivity of a new Pt(II) pentanuclear macrocycle bearing four cisplatin-like functionalities and its related monoplatinated specie. *J. Porphyrins Phthalocyanines* **2011,** *15*, 984-994. (d) Donzello, M. P.; Viola, E.; Ercolani, C.; Fu, Z.; Futur, D.; Kadish, K. M. Tetra-2,3-pyrazinoporphyrazines with Externally Appended Pyridine Rings. 12. New Heteropentanuclear Complexes Carrying Four Exocyclic Cis-platin-like Functionalities as Potential Bimodal (PDT/Cis-platin) Anticancer Agents. *Inorg. Chem.* **2012,** *51*, 12548-12559.

(3) (a) Manet, I.; Manoli, F.; Donzello, M. P.; Viola, E.; Andreano, G.; Masi, A.; Cellai, L.; Monti, S. A cationic Zn^{II} porphyrazine induces a stable parallel G-quadruplex conformation in human telomeric DNA. *Org. Biomol. Chem.* **2011,** *9*, 684-688. (b) Manet, I.; Manoli, F.; Donzello, M. P.; Ercolani, C.; Vittori, D.; Cellai, L.; Masi, A.; Monti, S. Tetra-2,3-pyrazinoporphyrazines with Externally Appended

Pyridine Rings. 10. A Water-Soluble Bimetallic (Zn^{II}/Pt^{II}) Porphyrazine Hexacation as Potential Plurimodal Agent for Cancer Therapy:Exploring the Behavior as Ligand of Telomeric DNA G Quadruplex Structures. *Inorg. Chem.* **2011,** *50*, 7403-7411.

(4) Manet, I.; Manoli, F.; Donzello, M. P.; Viola, E.; Masi, A.; Andreano, G.; Ricciardi, G.; Rosa, A.; Cellai, L.; Ercolani, C.; Monti, S. Pyrazinoporphyrazines with Externally Appended Pyridine Rings. 13. Structure, UV−Visible Spectral Features, and Noncovalent Interaction with DNA of a Positively Charged Binuclear (Zn^{II}/Pt^{II}) Macrocycle with Multimodal Anticancer Potentialities. *Inorg. Chem.* **2013,** *52*, 321-328.

(5) (a) Donzello, M. P.; Ou, Z.; Dini, D.; Meneghetti, M.; Ercolani, C.; Kadish, K. M. Tetra-2,3-pyrazinoporphyrazines with Externally Appended Pyridine Rings. 2. Metal Complexes of Tetrakis-2,3-[5,6-di(2-pyridyl)pyrazino]porphyrazine: Linear and Nonlinear Optical Properties and Electrochemical Behavior. *Inorg. Chem.* **2004**, *43*, 8637-8648. (b) Bergami, C.; Donzello, M. P.; Monacelli, F.; Ercolani, C.; Kadish, K. M. Tetra-2,3-pyrazinoporphyrazines with Externally Appended Pyridine Rings. 4. UV-Visible Spectral and Electrochemical Evidence of the Remarkable Electron-Deficient Properties of the New Tetrakis-2,3-[5,6-di{2-(N-methyl)pyridiniumyl}pyrazino]porphyrazinatometal Octacations, [(2-Mepy)$_8$TPyzPzM]$^{8+}$ (M = Mg^{II}(H_2O), Co^{II}, Cu^{II}, Zn^{II}). *Inorg. Chem.* **2005,** *44*, 9862-9873. (c) Donzello, M. P.; Viola, E.; Cai, X.; Mannina, L.; Rizzoli, C.; Ricciardi, G.; Ercolani, C.; Kadish, K. M.; Rosa, A. Tetra-2,3-pyrazinoporphyrazines with Externally Appended Pyridine Rings. 5. Synthesis, Physicochemical and Theoretical Studies of a Novel Pentanuclear Palladium(II) Complex and Related Mononuclear Species. *Inorg. Chem.* **2008,** *47*, 3903-3919. (d) Donzello, M. P.; Viola, E.; Xiaohui, C.; Mannina, L.; Ercolani, C.; Kadish, K. M. Tetra-2,3-pyrazinoporphyrazines with Externally Appended Pyridine Rings. 8. Central (Zn^{II}, Cu^{II}, Mg^{II}(H_2O), Cd^{II}) and Exocyclic (Pd^{II}) Metal Ion Binding in Heteropentametallic Complexes from Tetrakis-2,3-[5,6-di(2-pyridyl)pyrazino] porphyrazine. *Inorg. Chem.* **2010**, *49*, 2447-2456.

(6) Donzello, M. P.; De Mori, G.; Viola, E.; Ercolani, C.; Ricciardi, G.; Rosa, A. Tetra-2,3 pyrazinoporphyrazines with Externally Appended Pyridine Rings. 15. Effects of the Pyridyl Substituents and Fused Exocyclic Rings on the UV−Visible Spectroscopic Properties of Mg(II)-

Porphyrazines: A Combined Experimental and DFT/TDDFT Study. *Inorg. Chem.* **2014**, *53*, 8009-8019.

(7) Piechucki, C.; Michalski, *J. Bull. Acad. Polym. Sci., Ser. Sci. Chim.* **1970**, 18, 605.

(8) Donzello, M. P.; Viola, E.; Giustini, M.; Ercolani, C.; Monacelli, F. Tetrakis(thiadiazole)porphyrazines. 8. Singlet oxygen production, fluorescence response and liposomal incorporation of tetrakis(thiadiazole) porphyrazine macrocycles [TTDPzM] (M = Mg^{II}(H$_2$O), Zn^{II}, Al^{III}Cl, Ga^{III}Cl, Cd^{II}, Cu^{II}, 2H^{I}). *Dalton Trans.* **2012**, *41*, 6112-6121.

(9) Donzello, M. P.; Ou, Z. P.; Monacelli, F.; Ricciardi, G.; Rizzoli, C.; Ercolani, C.; Kadish, K. M. Tetra-2,3-pyrazinoporphyrazines with Externally Appended Pyridine Rings. 1. Tetrakis-2,3-[5,6-di(2-pyridyl)pyrazino]porphyrazine: A New Macrocycle with Remarkable Electron-Deficient Properties. *Inorg. Chem.* **2004,** *43*, 8626-8636.

(10) Velasquez, S. V.; Fox, G. A.; Broderick, W. E.; Andersen, K. A.; Anderson, O. P.; Barret, A. G. M.; Hoffman, B. M. star-Porphyrazines: synthetic, structural, and spectral investigation of complexes of the polynucleating porphyrazine octathiolato ligand. *J. Am. Chem. Soc.* **1992**, *114*, 7416-7424.

(11) Goslinski, T.; Tykarska, E.; Szczolko, W.; Osmalek, T.; Smigielska, A.; Walorczyk, S.; Zong, H.; Gdaniec, M.; Hoffman, B. M.; Mielcarek, J.; Sobiak, S. Synthesis and characterization of periphery-funcionalized porphyrazines containing mixed pyrrolyl and pyridylmethylamino groups. *J. Porphyrins Phthalocyanines* **2009**, *13*, 223-234.

(12) Baum, S. M.; Trabanco, A. A.; Montalban, A. G.; Micallef, A. S.; Zhong, C.; Meunier, H. G.; Suhling, K.; Phillips, D.; White, A. J. P.; Williams, D. J.; Barrett, A. G. M.; Hoffman, B. M. Synthesis and Reactions of Aminoporphyrazines with Annulated Five- and Seven-Membered Rings. *J. Org. Chem.* **2003,** *68*, 1665-1670.

(13) Templeton, D. H.; Fischer, M. S.; Zalkin, A.; Calvin, M. Structure and chemistry of the porphyrins. Crystal and molecular structure of the monohydrated dipyridinated magnesium phthalocyanine complex. *J. Am. Chem. Soc.* **1971,** *93*, 2622-2628.

(14) Matzumoto, S.; Endo, A.; Mizuguchi, J. Structure of magnesiumphthalocyanine complexes. Z. *Krystallogr.* 2000, *215*, 182-186.

(15) (a) Stuzhin, P.A.; Bauer, E. M.; Ercolani, C. Tetrakis(thiadiazole)porphyrazines. 1. Syntheses and Properties of Tetrakis(thiadiazole)porphyrazine and Its Magnesium and Copper Derivatives. *Inorg. Chem*. 1998, *37*, 1533-1539. (b) Bauer, E. M.; Ercolani, C.; Galli, P.; Popkova, I. A.; Stuzhin, P. A. Tetrakis(selenodiazole)porphyrazines.1: Tetrakis(selenodiazole)porphyrazine and its Mg(II) and Cu(II) derivatives. Evidence for their conversion to tetrakis(pyrazino)porphyrazines through octaaminoporphyrazines. *J. Porphyrins Phthalocyanine* 1999, *3*, 371-379.

(16) (a) Stuzhin, P. A.; Hamdush, M.; Ziener, U. Iron octaphenyltetraazaporphyrins: synthesis and characterization of the five-coordinate complexes of iron(III) (XFe^{III}OPTAP; X = F, Cl, Br, I, HSO$_4$). Inorg. Chim. Acta **1995**, *236*, 131-139. (b) Stuzhin, P.A.; Vagin, S. I.; Hanack, M. Synthesis and Spectral Properties of Bisaxially Coordinated (Octaphenyltetraazaporphyrinato)ruthenium(II) Complexes. *Inorg. Chem*. **1998**, *37*, 2655-2662.

(17) Berezin, B. D.; Khelevina, O. G.; Gerasimova, N. D.; Stuzhin, P. A. Kinetics of the Formation of Octaphenyltetra-azaporphin Compexes in Solution in Pyridine. *Russian Journal of Physical Chemistry* **1982**, *56*, 1699-1702.

(18) (a) Mack, J.; Stillman, M. J. in *The Porphyrin Handbook*; Kadish, K.M., Smith, K. M., Guilard, R., Eds.; Academic Press: New York, 2003; Vol. 16, pp 43-116. (b) Gouterman, M. In *The Porphyrins*; Dolphin, D., Ed.; Academic Press: New York, 1978; Vol. III, and references therein.

(19) (a) Electronic Spectra of Phthalocyanines and Related Compounds.Catalogue; Luk'yanets, E. A., Ed.; NIITEKhIM: Cherkassy, 1989; 94 pages (in Russian). (b) Kobayashi, N.; Konami, H. In Phthalocyanines - Properties and Applications; Leznoff, C. C., Lever, A. B. P., Eds.; VCH Publisher: New York, 1989; Vol. 4, pp 343−404.

(20) Donzello, M. P.; Dini, D.; D'Arcangelo, G.; Ercolani, C.; Zhan, R.; Ou, Z.; Stuzhin, P. A.; Kadish, K. M. Porphyrazines with Annulated Diazepine Rings. 2. Alternative Synthetic Route to Tetrakis-2,3-(5,7-diphenyl-1,4-diazepino)porphyrazines: New Metal Complexes, General Physicochemical Data, Ultraviolet-Visible Linear and Optical Limiting Behavior, and Electrochemical and Spectroelectrochemical Properties. *J. Amer. Chem. Soc.* **2003,** *125*, 14190-14204.

(21) De Mori, G.; Fu, Z.; Viola, E.; Cai, X.; Ercolani, C.; Pia Donzello, M.; Kadish, K. M. Tetra-2,3-pyrazinoporphyrazines with Externally Appended Thienyl Rings: Synthesis, UV_Visible Spectra, Electrochemical Behavior, and Photoactivity for the Generation of Singlet Oxygen *Inorg. Chem.* **2011,** *50*, 8225-8237.

(22) (a) Lever, A. B. P.; Wilshire, J. P. Redox potentials of metal phthalocyanines in non-aqueous media. *Canadian Journal of Chemistry* **1976,** *54*, 2514-2516. (b) Giraudeau, A.; Fan, F.-R. F.; Bard, A. J. Semiconductor electrodes. 30. Spectral sensitization of the semiconductors titanium oxide (n-TiO$_2$) and tungsten oxide (n-WO$_3$) with metal phthalocyanines. *J. Am. Chem. Soc.* **1980,** *102*, 5137-5142. (c) Shao, J.; Commodore, J.; Han, B.; Pruente, C.; Hansen, C. A. Electrochemical, spectroelectrochemical and ESR spectroscopic characterization of 2,3- and 3,4-cobalt tetrapyridoporphyrazine isomers in non-aqueous media. *J. Porphyrins Phthalocyanines* **2009,** *13*, 876-887. (d) Mashazi, P.; Antunes, E.; Nyokong, T. Probing electrochemical and electrocatalytic properties of cobalt(II) and manganese(III) octakis(hexylthio)phthalocyanine as self-assembled monolayers. *J. Porphyrins Phthalocyanines* **2010,** *14*, 932-947.

(23) (a) Truxillo, L. A.; Davis, D. G. Electrochemistry of cobalt tetraphenylporphyrin in aprotic media. *Analytical Chemistry* **1975**, *47*, 2260-2267. (b) Walker, F. A.; Beroiz, D.; Kadish, K. M. Electronic effects in transition metal porphyrins. 2. The sensitivity of redox and ligand addition reactions in para-substituted tetraphenylporphyrin complexes of cobalt(II)**.** *J. Am. Chem. Soc.* **1976**, *98*, 3484-3489.

(24) (a) Moreira, L. M.; Vieira dos Santos, F.; Pereira Lyon, J.; Maftoum-Costa, M.; Pacheco-Soares, C.; Soares da Silva, N. Photodynamic Therapy: Porphyrins and Phthalocyanines as Photosensitizers. *Aust. J. Chem.* **2008**, *61*, 741-754. (b) O'Connor, A. E.; Gallagher, W. M.; Byrne, A. T. Porphyrin and Nonporphyrin Photosensitizers in Oncology: Preclinical and Clinical Advances in Photodynamic Therapy. *Photochem. Photobiol.* **2009,** *85*, 1053-1074.

(25) (a) Shinohara, H.; Tsaryova, O.; Schnurpfeil, G.; Wöhrle, D. Differently substituted phthalocyanines: Comparison of calculated energy levels, singlet oxygen quantum yields, photo-oxidative stabilities, photocatalytic and catalytic activities. *J. Photochem. Photobiol. A*: *Chemistry* **2006***, 184*, 50-57.(b) Spiller, W.; Kliesch, H.; Wöhrle, D.; Hackbarth, S.; Röder, B.; Schnurpfeil, G.

Singlet oxygen quantum yields of different photosensitizers in polar solvents and micellar solutions. *J. Porphyrins Phthalocyanines* **1998**, *2*, 145-158. (c) Schnurpfeil, G.; Sobbi, A. K.; Spiller, W.; Kliesch, H.; Wöhrle, D. Photo-oxidative Stability and its Correlation with Semi-empirical MO Calculations of Various Tetraazaporphyrin Derivatives in Solution. *J. Porphyrins Phthalocyanines* **1997**, *1*, 159-167. (d) Fernandez, D. A.; Awruch, J.; Dicelio, L. E. Photophysical and Aggregation Studies of t-Butyl-Substituted Zn Phthalocyanines. *Photochem. Photobiol.* **1996**, *63*, 784-792. (e) Müller, S.; Mantareva, V.; Stoichkova, N.; Kliesch, H.; Sobbi, A.; Wöhrle, D.; Shopova, M. Tetraamido-substituted 2,3-naphthalocyanine zinc(II) complexes as phototherapeutic agents: synthesis, comparative photochemical and photobiological studies. *J. Photochem. Photobiol. B: Biology* **1996**, *35*, 167-174. (f) Maree, S. E.; Nyokong, T. Syntheses and photochemical properties of octasubstituted phthalocyaninato zinc complexes. *J. Porphyrins Phthalocyanines* **2001**, *5*, 782-792. (g) Lawrence, D.S.; Whitten, D. G. Photochemistry and Photophysical Properties of Novel, Unsymmetrically Substituted Metallophthalocyanines. *Photochem. Photobiol.* **1996**, *64*, 923-935.

(26) Machacek, M.; Cidlina, A.; Novakova, V.; Svec, J.; Rudolf, E.; Miletin, M.; Kučera, R.; Simunek, T.; Zimcik, P. Far-Red-Absorbing Cationic Phthalocyanine Photosensitizers: Synthesis and Evaluation of the Photodynamic Anticancer Activity and the Mode of Cell Death Induction. *J. Med. Chem.* **2015**, *58*, 1736-1749.

 (27) Nyokong, T. Effects of substituents on the photochemical and photophysical properties of main group metal phthalocyanines. *Coord. Chem. Rev.* **2007**, *251*, 1707-1722.

 (28) (a) Musil, Z.; Zimcik, P.; Miletin, M.; Kopecky, K.; Petrik, P.; Lenco, J. Influence of electron-withdrawing and electron-donating substituents on photophysical properties of azaphthalocyanines. J. Photochem. Photobiol., A: Chemistry **2007**, *186*, 316-322. (b) Baum, S. M.; Trabanco, A. A.; Montalban, A. G.; Micallef, A. S.; Zhong, C.; Meunier, H. G.; Suhling, K.; Phillips, D.; White, A. J. P.; Williams, D. J.; Barrett, A. G. M.; Hoffman, B. M. Synthesis and Reactions of Aminoporphyrazines with Annulated Five- and Seven-Membered Rings. *J. Org. Chem.* **2003**, *68*, 1665-1670. (c) Sakellariou, E. G.; Montalban, A. G.; Meunier, H.; Rumbles, G.; Philips, D.; Ostier, R. B.; Suhling, K.; Barrett, A. G. M.; Hoffman, B. M. Peripherally Metalated Secoporphyrazines: A New Generation of

Photoactive Pigments. *Inorg. Chem*. **2002,** *41*, 2182-2187. (d) Montalban, A. G.; Baum, S. M.; Barrett, A. G. M.; Hoffman, B. M. Studies on seco-porphyrazines: a case study on serendipity. *Dalton Trans*. **2003**, *40*, 2093-2102. (e) Michelsen, U.; Kliesch, H.; Schnurpfeil, G.; Sobbi, A. K.; Wöhrle, D. Un symmetrica My Substituted Benzonaphthoporphyrazines: A New Class of Cationic Photosensitizers for the Photodynamic Therapy of Cancer. *Photochem. Photobiol*. **1996**, *64*, 694-701. (f) Dumoulin, F.; Durmus, M.; Ahsen, V.; Nyokong T. Synthetic pathways to water-soluble phthalocyanines and close analogs. *Coord. Chem. Rev*. **2010**, *254*, 2792-2847.

Synopsis

Synthesis, UV-visible spectra, electrochemistry and photoactivity in PDT of octakis(2-pyridyl)porphyrazine, [Py_8PzH_2], and its metal derivatives [Py_8PzM] ($M = Mg^{II}(H_2O)$, Co^{II}, Cu^{II}, Zn^{II}) are reported.